# MITOCHONDRIAL GENOME SEQUENCING AND ANALYSIS OF THE INVASIVE *MICROSTEGIUM VIMINEUM*: A RESOURCE FOR SYSTEMATICS, INVASION HISTORY, AND MANAGEMENT

Craig F. Barrett,[1,*] Dhanushya Ramachandran,* Chih-Hui Chen,† Cameron W. Corbett,* Cynthia D. Huebner,*,‡,§ Brandon T. Sinn,‖,# Wen-Bin Yu,** and Kenji Suetsugu††

*Department of Biology, West Virginia University, 53 Campus Drive, Morgantown, West Virginia 26506, USA; †Endemic Species Research Institute, 1 Ming-Sheng East Road, Jiji, Nantou 552, Taiwan; ‡USDA Forest Service, Northern Research Station, 180 Canfield Street, Morgantown, West Virginia 26505, USA; §Division of Plant and Soil Sciences, West Virginia University, 204 Evansdale Greenhouse, Morgantown, West Virginia 26505, USA; ‖Department of Biology and Earth Science, Otterbein University, 1 South Grove Street, Westerville, Ohio 43081, USA; #Faculty of Biology, University of Latvia, 1 Jelgavas iela, Riga, Latvia LV-1004; **Center for Integrative Conservation, Xishuangbanna Tropical Botanical Garden, Chinese Academy of Sciences, Mengla, Yunnan 666303, China; and †† Department of Biology, Graduate School of Science, Kobe University, 1-1 Rokkodai, Nada-ku, Kobe 657-8501, Japan

*Editor: Jeremie Fant*

*Premise of research*. Plants remain underrepresented among species with sequenced mitochondrial genomes (mitogenomes) because of the difficulty in assembly with short-read technology. Invasive species lag behind crops and other economically important species in this respect, resulting in a lack of tools for management and land conservation efforts.

*Methodology*. The mitogenome of *Microstegium vimineum*, one of the most damaging invasive plant species in North America, was sequenced and analyzed using long-read data, providing a resource for biologists and managers. We conducted analyses of genome content, phylogenomic analyses among grasses and relatives based on mitochondrial coding regions, and an analysis of mitochondrial single-nucleotide polymorphism in this invasive grass species.

*Pivotal results*. The assembly is 478,010 bp in length and characterized by two large inverted repeats and a large direct repeat. However, the genome could not be circularized, arguing against a "master circle" structure. Long-read assemblies with data subsets revealed several alternative genomic conformations, predominantly associated with large repeats. Plastid-like sequences comprise 2.4% of the genome, with further evidence of class I and class II transposable element-like sequences. Phylogenetic analysis placed *M. vimineum* with other *Microstegium* species, excluding *Leptathera* (*Microstegium*) *nudum*, but with weak support. Analysis of polymorphic sites across 112 accessions of *M. vimineum* from the native and invasive ranges revealed a complex invasion history.

*Conclusions*. We present an in-depth analysis of mitogenome structure, content, phylogenetic relationships, and range-wide genomic variation in *M. vimineum*'s invasive US range. The mitogenome of *M. vimineum* is typical of other andropogonoid grasses, yet mitochondrial sequence variation across the invasive and native ranges is extensive. Our findings suggest multiple introductions to the US over the last century, with subsequent spread, secondary contact, long-distance dispersal, and possible postinvasion selection on awn phenotypes. Efforts to produce genomic resources for invasive species, including sequenced mitochondrial genomes, will continue to provide tools for their effective management and to help predict and prevent future invasions.

*Keywords:* invasion genomics, mitogenome, long-read sequencing, grass, Poaceae.

*Online enhancements:* supplemental figures, table.

[1] Author for correspondence; email: craig.barrett@mail.wvu.edu.
**ORCIDs:** Barret, https://orcid.org/0000-0001-8870-3672.

*Manuscript received February 2023; revised manuscript received February 2023; electronically published August 18, 2023.*

## Introduction

Invasive species cause damage to natural, agricultural, and urban ecosystems, amounting to billions of dollars in economic

 © 2023 The University of Chicago. All rights reserved. Published by The University of Chicago Press. https://doi.org/10.1086/726005

and environmental loss (Pimentel et al. 2005; Simberloff et al. 2013). Such problems have been exacerbated by climate change and greater interconnectedness across the globe (Finch et al. 2021). Genomic resources provide practitioners and researchers with a baseline of powerful tools in medicine, agriculture, and virtually all areas of the life sciences, yet such tools are generally lacking for invasive species compared to those in crop and animal systems (Matheson and McGaughran 2022). However, the widespread availability and increasing affordability of genome sequencing technologies and bioinformatic platforms are changing the landscape of invasion biology (North et al. 2021). For example, such advances in genomics are allowing more nuanced reconstructions of invasion history (van Boheemen et al. 2017; Sutherland et al. 2021; Bieker et al. 2022), linking of genotypic and phenotypic variation (Turner et al. 2021; Revolinski et al. 2023), epigenetics (Banerjee et al. 2019; Mounger et al. 2021), and forecasting of potential future invasions (Hudson et al. 2021).

Generally speaking, plant mitochondrial genomes (mitogenomes) have experienced less attention than plastid or nuclear genomes (Mower et al. 2012). This is largely because of their extensive variability in structural dynamics and repetitive DNA content, making them difficult targets for complete genomic sequencing (Palmer and Herbon 1988; Alverson et al. 2010). This is in contrast to animal mitogenomes, which evolve rapidly in terms of substitution rates but are more structurally conserved. In combination with their smaller size (10–20 kb in animals vs. 100 kb to >10 Mb in plants; Gualberto et al. 2014), animal mitogenome sequencing is more straightforward than in plants, making animal mitogenomes significantly better represented across the Tree of Life. Improvements in long-read sequencing technology, however, have allowed the assembly of complete or nearly complete mitogenomes and have renewed interest in plant mitochondrial genomics (Kovar et al. 2018; Jackman et al. 2020). Analyses of plant mitogenomes have revealed an array of structures, including circular genomes, substoichiometric circular structures, linear structures, multichromosomal structures, and branched structures (Bendich 1993; Sloan 2013; Wu et al. 2015, 2022).

Plant mitogenomes typically contain 50–60 genes, including those encoding protein products (coding DNA sequences [CDS]), transfer RNAs (tRNAs), and ribosomal RNAs (rRNAs; Gualberto et al. 2014). They are also known to contain plastid-like regions, likely as remnants of both ancient and recent intergenomic transfers and gene conversion events; such regions represent up to 10.3% of the mitogenome in the date palm *Phoenix dactylifera* L. (Fang et al. 2012). Additionally, plant mitogenomes have been demonstrated to house foreign DNA, possibly remnants of ancient or more recent close biotic interactions (e.g., Rice et al. 2013; Sanchez-Puerta et al. 2017; Sinn and Barrett 2020; Lin et al. 2022).

Grass mitogenomes have received more attention than those in most other plant families, with 67 complete genomes in National Center for Biotechnology Information (NCBI) GenBank, though more than half of these comprise multiple accessions of a few crop species (e.g., *Hordeum vulgare* L., *Oryza sativa* L., *Triticum aestivum* L., *Zea mays* L.). However, grass species are also overrepresented among invasive plant species overall compared to most other flowering plant families (Daehler 1998; Kerns et al. 2020), allowing for meaningful comparisons among invasive and noninvasive species within this ecologically and economically important family. Only a handful of mitogenomes have been sequenced for invasive plants (e.g., *Silene vulgaris* (Moench) Garcke (Caryophyllaceae)), and most are grasses (e.g., *Chrysopogon zizianoides* (L.) Roberty, *Coix lacryma-jobi* L., *Eleusine indica* (L.) Gaertn., and *Lolium perenne* L. (Poaceae)). Thus, studies of mitochondrial genome dynamics in invasive plants are in their infancy, as are potential applications in their effective control. For example, a simulation study by Hodgins et al. (2009) explored the possibility of incorporating cytoplasmic (mitochondrial) male sterility alleles in the control of invasive plants by limiting pollen production. To date, empirical data and sequenced reference mitogenomes are too few to test the effectiveness of such approaches more broadly in invasive plant species, nearly all of which can be categorized as nonmodel species.

*Microstegium vimineum* (Trin.) A. Camus (Poaceae: Panicoideae: Andropogoneae; stiltgrass) is an aggressive, established invader of eastern North American forest ecosystems (e.g., Huebner 2010*a*; Johnson et al. 2015; Soreng et al. 2022). Likely introduced as packing material for porcelain in the early 1900s (Fairbrothers and Gray 1972), this polyploid species (2n = 20) has spread to 30 US states and is expanding into Canada, the northeastern US, and the upper Midwest (Mortensen et al. 2009; Huebner 2010*a*, 2010*b*; Rauschert et al. 2010; Barrett et al. 2022). Further, it is hypothesized that *M. vimineum* was introduced multiple times in the US, first in the southeastern US, and later in the Northeast, with subsequent spread and secondary contact, providing an apt case study in the genomic dynamics of the invasion process (Novy et al. 2013; Barrett et al. 2022). Recently published plastid and nuclear genomes are now available for this species (respectively, Welker et al. 2020; Ramachandran et al. 2021), but a complete mitogenome is lacking. Therefore, the objective of this study is to assemble a reference mitogenome for *M. vimineum*, with the goal of aiding studies of invasion history, evolution, ecology, and management. We explore genome structure and content, phylogenetic relationships of *Microstegium* Lindb., and patterns of mitogenomic variation across the native and invasive ranges with respect to invasion history in *M. vimineum*.

## Material and Methods

### *Organellar Genome Sequencing and Assembly*

Leaf material was sampled from a growth chamber–grown accession (seed from Potomac Ranger District, Monongahela National Forest, West Virginia), flash-frozen in liquid nitrogen, and stored at −80°C. DNAs/RNAs were extracted, and PacBio (DNA) and Illumina (DNA and RNA) sequencing were conducted as described in Ramachandran et al. (2021). The software seqtk version 1.0-r31 (https://github.com/lh3/seqtk) was used to randomly subsample PacBio reads (400,000 reads). MegaBLAST from the NCBI BLAST+ suite (Camacho et al. 2009) was conducted with the subsampled read pools against the mitochondrial genome of *Sorghum bicolor* (L.) Moench (NCBI GenBank no. NC_008360) in Geneious version 10.0.9 (http://www.geneious.com/), specifying an *e*-value of $1e^{-5}$, keeping reads >20 kb in length, and binning them into "hits" and "no hits." The resulting positive BLAST hits for each set were then assembled with CANU version 2.2 under default parameters

(Koren et al. 2017). The resulting graphs from CANU (.gfa files) were inspected in BANDAGE version 0.9.0 (Wick et al. 2015) to visualize contiguity and coverage of the assemblies. Resulting scaffolds were further assembled into a single scaffold in Geneious using the native overlap-layout-consensus "*de novo* assembly" option. Mitochondrial and plastid contigs were identified using the live annotation feature in Geneious, with the annotations from *S. bicolor* (mitochondrial) and an accession of *Microstegium vimineum* (plastome; accession TK124, GenBank no. MT610045) at a 70% threshold, respectively. Circlator was used to attempt to circularize the scaffold (Hunt et al. 2015).

Mitochondrial and plastid contigs were extracted separately as FASTA files. FLYE was then used to correct the mitochondrial and plastid scaffolds with 10 polishing iterations using the PacBio data (Kolmogorov et al. 2019). The assembly was further polished with Illumina data using PILON (Walker et al. 2014). Illumina data (8,605,412 read pairs from accession WV-PRD-2-4, the same collection used for PacBio sequencing) were trimmed with BBDUK version 38.51 (https://sourceforge.net/projects/bbmap) to remove Illumina adapters, low-quality bases (minimum quality = 6), and low-complexity regions (minimum entropy = 0.5, maximum GC content = 0.9). Illumina reads were then mapped to the organellar assemblies with NGM (Sedlazeck et al. 2013) to output a .sam alignment file. The .sam file was then sorted and indexed with SAMTOOLS version 1.7 (Li et al. 2009). The PacBio assemblies and sorted .bam file were then used for error correction/polishing with PILON.

The resulting polished FASTA file was imported into Geneious and annotated using the live annotation feature, at a 75% similarity threshold, using the mitochondrial annotations from *Coix lacryma-jobi* var. *ma yuen* (Rom. Caill.) Stapf ex Hook. f. (GenBank accession no. MT471100), *S. bicolor* (NC_008360), *Oryza sativa* (ON854123), *Zea mays* (CM025451), and *Saccharum officinarum* L. (MG969496), along with the plastid annotation from *M. vimineum* (MT610045). Annotations were then checked visually to confirm proper start/stop codons and to investigate the presence of premature stop codons, suggesting misannotations. The annotation was exported from Geneious as a GenBank Flat File and converted to a feature table with GB2Sequin (Lehwark and Greiner 2019) via the ChloroBox portal (https://chlorobox.mpimp-golm.mpg.de). The resulting feature table was downloaded and manually edited to ensure the correct orientation of exons in genes containing them. The annotation (feature table + FASTA file) was then submitted to GenBank though the BankIt web portal (https://www.ncbi.nlm.nih.gov/WebSub).

### *Analyses of Repetitive DNA, Plastid-Like DNA, RNA Editing, and Structural Variation*

Geneious was used to identify large, identical repeats >1000 bp, using the native Repeat Finder plug-in (https://www.geneious.com/plugins/repeat-finder/) and the self-dotplot function, with a window size of 500 bp and tile size of 100 kb. REPuter (Kurtz et al. 2001; via https://bibiserv.cebitec.uni-bielefeld.de/reputer/) was further used to detect repetitive regions >8 bp in length in forward, reverse, reverse-complement, and palindromic configurations (edit and Hamming distances = 0). Plastid-like regions were identified by annotating the mitogenome with all plastid genes from *M. vimineum* (GenBank accession no. MT610045) in Geneious at a 60% similarity threshold, in order to detect degraded or pseudogenized plastid-like sequences. Further, to identify plastid-like regions not corresponding to annotated genes, Illumina reads from accession WV-PRD-2-4 (MT610045) were mapped to the reference mitogenome to identify putative plastid-like regions with higher than expected coverage depth. These regions were annotated in Geneious as having >3 × standard deviations in coverage depth relative to the rest of the genome.

RNAseq reads from the same collection, made from young, developing leaf tissue (NCBI Sequence Read Archive accession no. SRX12501806), were mapped to the reference genome using the Geneious read mapper for RNAseq data, and single-nucleotide polymorphisms (SNPs) were called to identify putative RNA editing sites for all CDS (e.g., C to U). Minimum required coverage depth for a SNP was 10 × , further requiring a minimum variant frequency of 0.9, such that only variants that differed among the RNAseq and DNAseq data were identified (i.e., the polished reference). Relative expression levels (transcripts per million [TPM]) were calculated in two ways. First, all RNAseq reads were mapped to the plastome to filter plastid reads in Geneious, then the remaining reads were mapped to the mitochondrial annotation to quantify expression levels of all mitochondrial CDS. The plastid-like region annotations were overlaid on the mitochondrial genomes, and plastid-filtered reads were mapped to assess whether plastid-like regions of the mitogenome displayed evidence of expression. All results were plotted in R with the packages dplyr version 1.0.10 (Wickham et al. 2023), ggplot2 version 3.3.6 (Wickham 2016), and ggpubr version 0.4.0 (Kassambara 2020). To investigate variation in mitogenome structure, eight random subsets of 200,000 PacBio reads were sampled with Seqtk and BLASTed against the *Sorghum* mitogenome (as above). BLAST hits were assembled with FLYE, and the longest mitochondrial contigs were mapped to the reference genome model with the LASTZ version 1.04.22 (Harris 2007) plug-in for Geneious.

### *Identification of Transposable Elements and Foreign-Acquired Sequence*

RepeatMasker version 4.1.1 (Smit et al. 2013) was used to discover and identify transposable elements (TEs) in the mitogenome assembly, using the RepBase-20181026 database of Viridiplantae (Bao et al. 2015) and a custom set of 1279 *M. vimineum* consensus repeat sequences (Ramachandran et al. 2021). Additional repeat identification tools were used to screen for the presence of partial or truncated TE sequences in the mitogenome. HelitronScanner (Xiong et al. 2014) was used to identify helitrons using 5′ and 3′ terminal motifs. Miniature inverted-repeat transposable elements (MITEs) were detected using the program MiteFinderII (Hu et al. 2018) under default settings.

Kraken 2 (ver. 2.1.2; Wood et al. 2019) was used to screen for the presence of interspecific genomic transfers, excluding those from the plastome. The mitogenome assembly, with repeats masked and plastid sequences removed, was decomposed into 100-bp segments using the reformat.sh script of the BBMAP suite (https://sourceforge.net/projects/bbmap/). The resulting 4292 sequences were classified via screening against precompiled Kraken 2 databases (available via https://benlangmead.github.io

/aws-indexes/k2): (1) the PlusPFP database, which contained the complete genomes of plants, bacteria, archaea, viruses, fungi, human, and UniVec vectors accessioned in NCBI's RefSeq database and (2) the Eukaryotic Pathogen, Vector and Host Informatics Resource Database (Amos et al. 2022), which contained sequences from 389 species. The NCBI taxonomy was used for the annotation of classified sequences. The default values for *k*-mer length (35) and minimizer value (31) were used.

### *Phylogenomic Analyses Using Mitochondrial CDS*

Mitochondrial genomes and mitochondrial protein CDS were downloaded from NCBI GenBank, using the search terms "Poales," "mitochondrion," and "complete." *Cocos nucifera* L. (NC_031696) and *Phoenix dactylifera* (NC_016740) were chosen as outgroups, as both are members of the palm family (Arecales) and the commelinid clade, to which Poales also belongs. Sequence annotations were extracted from Geneious and aligned with the codon-aware aligner MACSE version 2 (Ranwez et al. 2018). Alignments were then concatenated in Geneious, and sites with >10% missing data were excluded (table S1). The final alignment was analyzed with maximum likelihood under the general heterogeneous evolution on a single topology (GHOST) heterotachy model (Crotty et al. 2020) in IQTree2 (Minh et al. 2020), which allows mixed substitution rates and branch lengths. This model is especially appropriate for lineages such as Poales, which have been shown in previous studies to exhibit heterotachy in phylogenomic estimates based on organellar DNA (e.g., Givnish et al. 2010; Barrett et al. 2016). This model approach avoids the need to partition the data by gene and codon and can accommodate changes in substitution rates across branches and time. IQTree2 was run under the GHOST model with 1000 ultrafast bootstrap pseudoreplicates (Hoang et al. 2018). The resulting tree file was visualized in FigTree version 1.4.4 (http://tree.bio.ed.ac.uk/) and edited with Adobe Illustrator version 26.5 (Adobe 2019).

### *Assessment of Relationships among Mitochondrial Haplotypes of* M. vimineum

To characterize haploid SNPs in the mitogenome, we sampled 112 accessions from both the invasive ($n = 74$) and native ranges (Asia, $n = 38$), plus six accessions from different species of *Microstegium* as outgroups. Samples were field collected either in 2019–2020 ($n = 66$) or from herbarium specimens ($n = 46$) dating back to 1934 and as recent as 2010 (appendix). Total genomic DNAs were extracted via the CTAB method (Doyle and Doyle 1987) and quantified via Qubit Broad Range DNA assay (Thermo Fisher Scientific, Waltham, MA). DNAs were further visualized on a 1% agarose gel to assess degradation and diluted to 20 ng/$\mu$L with nanopure water. Illumina sequencing libraries were prepared with the SparQ DNA Frag and Library Kit at 2/5 volume (Quantabio, Beverly, MA), which uses a fragmentase to shear genomic DNA, followed by end repair and adapter ligation. The shearing step for herbarium-derived DNAs was reduced to 1 min from 14 min, as these all showed some level of fragmentation prior to library preparation. Libraries were then amplified with primers matching the adapter sequences, adding dual-indexed barcodes (12 polymerase chain reaction [PCR] cycles). Final, barcoded library concentrations were determined via Qubit High Sensitivity DNA assay and pooled at equimolar ratios. Library pools were sequenced on two runs of 2 × 100 bp Illumina Nextseq2000 (ver. 3 chemistry) at the Marshall University Genomics core with samples from other studies, producing a total of ≈1 billion read pairs per run.

Reads were processed using a dedicated SNP calling pipeline (https://github.com/btsinn/ISSRseq; with scripts available at https://zenodo.org/record/5719146#.Y-EvfnbMKHs; Sinn et al. 2022). Briefly, reads were trimmed and filtered with BBDUK (http://sourceforge.net/projects/bbmap), with minimum read quality = PHRED 20, entropy and low-complexity filters set to remove reads with <0.1% or >0.9% GC content, *k*-mer length set to 18, and the "mink" flag set to 8. The reference genome was indexed and reads were mapped with BBMAP (https://sourceforge.net/projects/bbmap/). Here, plastid-like regions and one copy of each large repeat were removed from the reference genome to minimize drastic differences in coverage depth and plastid SNPs being misinterpreted as mitochondrial SNPs. The resulting .bam files were sorted and PCR duplicates were removed with PICARD (ver. 2.22.8; Broad Institute). SNPs were called with Genome Analysis Toolkit (GATK) HaplotypeCaller (Poplin et al. 2017) following GATK best practices (Van der Auwera et al. 2013; Van der Auwera and O'Connor 2020), here with ploidy = 1, resulting in .vcf files for all raw and GATK-filtered variants. The filtered .vcf was then converted to .nexus format with vcf2phylip (Ortiz 2019), keeping only sites represented in at least 12 accessions (fig. S2). Phylogenetic analysis was conducted as above, with the exception that the GHOST heterotachy model was not used (as variation below the species level should not be expected to show strong patterns of heterotachy). Instead, the best-fit model was selected from the entire dataset using ModelFinder (Kalyaanamoorthy et al. 2017) under the Bayesian information criterion (BIC).

The annotated mitogenome sequence for *M. vimineum* was deposited in NCBI GenBank under accession number OQ360108. Raw read data used to build the genome (PacBio, RNAseq), for phylogenomics, and for SNP analysis (DNAseq) were deposited in the NCBI Sequence Read Archive under BioProject PRJNA769079. Supplementary files are available at https://doi.org/10.5281/zenodo.7618370.

## Results

### *Organellar Genome Sequencing and Assembly*

The final, polished assembly was 478,010 bp in length (fig. 1*A*), with overall GC content at 43.7% (41.3% for protein-coding sequences, 53.0% for rRNA genes, and 51.1% for tRNA genes). The initial assembly resulted in six contigs, three of which comprised the plastid genome (large and small single-copy regions, inverted repeat [IR]) and three of which comprised the mitogenome. The latter were assembled into a single contig based on overlapping ends with the Geneious "de novo" assembler. Despite attempts to circularize the genome with Circlator, a single "master circle" model could not be constructed. The final genome assembly contained two large inverted repeats and a single, large direct repeat (DR): IR1 (28,247 bp), IR2 (2380 bp), and DR1 (6462 bp), respectively. Potential secondary structures

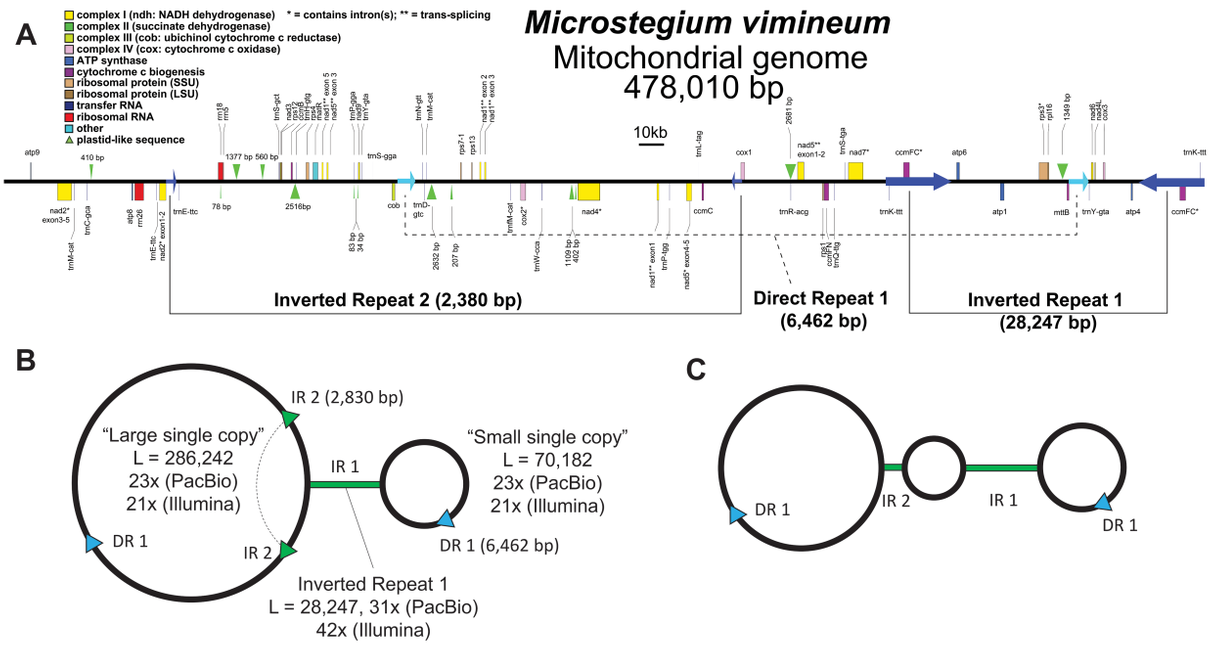


**Fig. 1** *A*, Linear map of the *Microstegium vimineum* mitogenome assembly and annotation. Scale = 10 kb. *B*, Proposed mitogenome secondary structural model emphasizing a single large inverted repeat. *C*, Proposed model emphasizing two large inverted repeats. IR = inverted repeat; DR = direct repeat; L = length of each region; *N*× = mean coverage depth of each region in *B*. Note that the genome in *B* and *C* is represented as a looped or circular structure, but the genome could not be circularized with long-read data.

of the genome model are depicted in figure 1*B*, 1*C*. One possible secondary structure (fig. 1*B*) consists of large and small single-copy regions (which contain copies of IR2 and DR1) and a large IR(1). Another possible structure, considering both large IR sequences, consists of three single-copy regions, separated by the two IRs (fig. 1*C*). Mean coverage depths of the three regions from figure 1*B* are: 31 × (PacBio) and 42 × (Illumina) for IR1 and 23 × (PacBio) and 21 × (Illumina) for the both single-copy regions.

### *Analyses of Repetitive DNA, Structural Variation, Plastid-Like DNA, RNA Editing, TEs, and Foreign-Acquired Sequences*

The genome assembly contains 32 CDS, three rRNA genes (*rrn*), and 27 tRNA genes (*trn*). In addition to the large repeat regions above, the mitogenome of *Microstegium vimineum* contains numerous smaller repeats (<1000 bp). These include DRs (880 bp, 262 bp, 164 bp, and 109 bp), IRs (165 bp, 109 bp), and one repeat with three intervals of 154 bp (forward, forward, reverse). The genome contains eight tandem repeat regions: $(AC)_6$, $(AG)_6$, $(AT)_{10}$, $(CT)_6$, $(ACTTT)_5$, and three regions of $(AT)_7$. Further, it contains 87 dispersed repeats <100 bp in length in forward/forward orientation (mean length = 36.3 bp) and 101 in forward/reverse orientation (mean length = 35.0 bp). Comparison of repeat content with relatives of *M. vimineum* within tribe Andropogoneae reveal similar patterns (fig. 2*A*): large IRs (>5 kb) are present in *M. vimineum* (2), *Chrysopogon zizanioides* (3), and *Coix lacryma-jobi* (4). The same is true for large DRs, which are present in all species: *Microstegium* (1), *Chrysopogon* (1), *Coix* (2), *Saccharum* (1), and *Sorghum* (2). LastZ alignments revealed seven different structural conformations of the *M. vimineum* mitogenome based on assemblies from eight random subsets of 200,000 PacBio reads (fig. 2*B*). Nearly all of the apparent breakpoints were associated with large DR or IR regions, while one major breakpoint was associated with a small (109-bp) DR.

Plastid-like sequences comprise 2.4% of the genome. In total, successfully transferred annotations of plastid genes to the mitogenome comprised 43 annotations, 17 of which were CDS (fig. 3) and the remainder of which were tRNA-like genes. Average percent similarity for CDS was 78.53 (range = 39.7) and for *trn*-like regions was 76.01 (range = 39.2). The three largest annotated plastid-like regions in the *M. vimineum* mitogenome correspond to *atpB*, *psaB*, and *rpoC1*, with percent similarities to their plastomic homologs of 75.3, 73.6, and 70.9, respectively (fig. 3). Several plastid-like sequences are also found in the mitogenomes of other members of tribe Andropogoneae and more broadly among grasses, including *atpB, atpE, ndhK, psaB, psbF, rpl14, rpl2, rpl23, rpoC1, rps19*, and *rps2*. All plastid-like mitochondrial regions in *M. vimineum* showed evidence of pseudogenization relative to their plastid-encoded homologs, including high levels of divergence, 5′ or 3′ truncation, internal stop codons, and frameshift insertions or deletions. The only region with an intact reading frame corresponded to *atpE*, having three substitutional differences relative to the plastid copy; two of these were adjacent and resulted in replacements at codons 3 and 4 (L → F and N → H, respectively).

Analyses of gene expression based on RNA-seq data from developing leaf tissue revealed that over half of all expressed mitochondrial

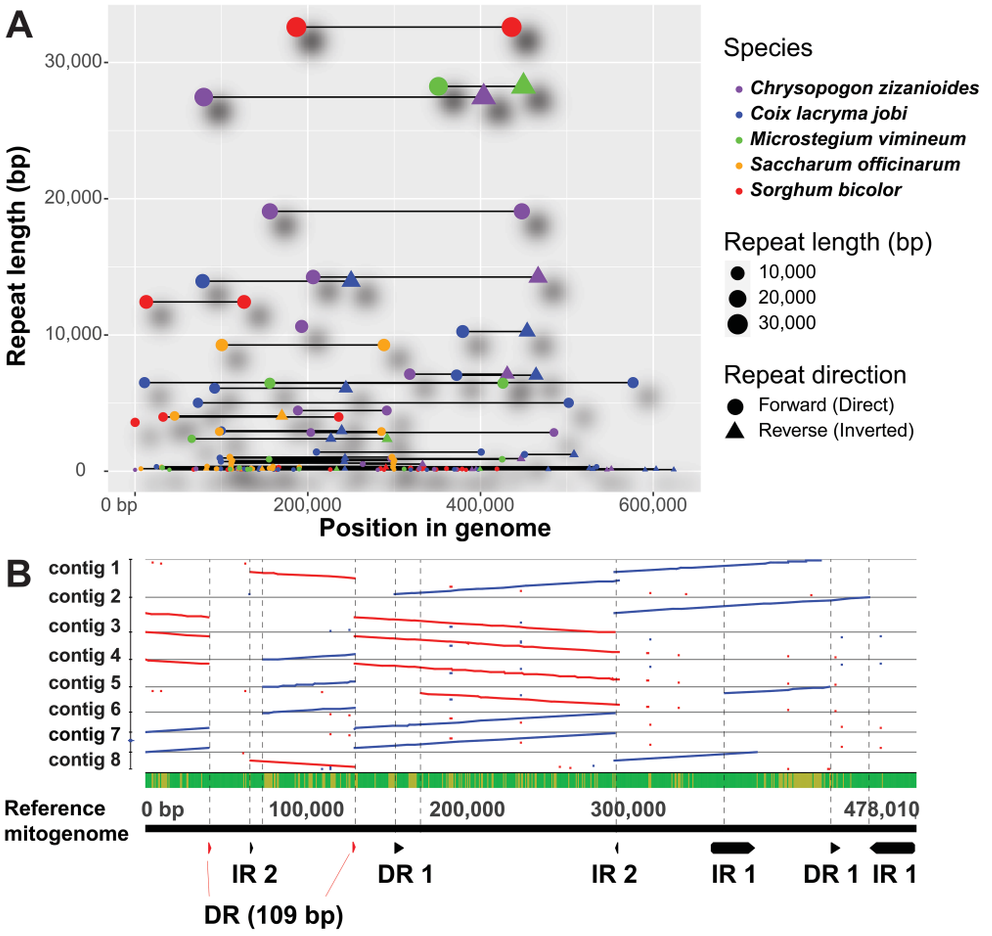


**Fig. 2** *A*, Repeat distribution in the mitogenomes of five species of grasses within the tribe Andropogoneae. Points represent repeats scaled by size; shapes represent the orientation of each repeat. *B*, Alternative conformations of the mitogenome based on LASTZ alignments of assemblies of eight randomized subsets of PacBio reads, relative to the genome model in figure 1*A*. IR = inverted repeat; DR = direct repeat; red lines = forward orientation; blue lines = reverse orientation.

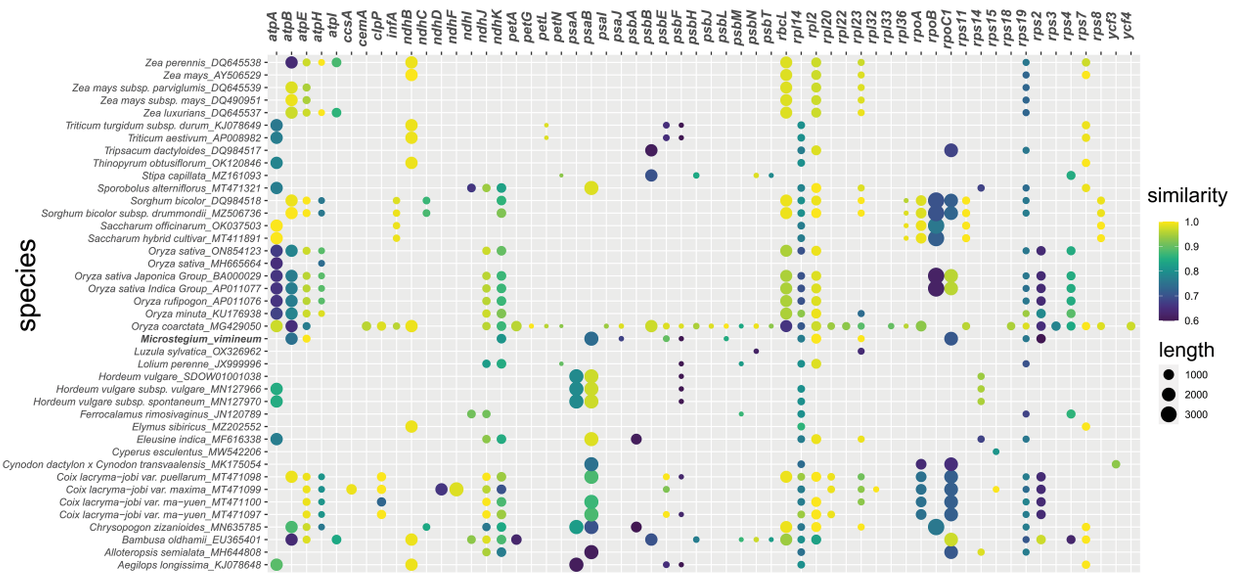


**Fig. 3** Plastid-like sequences in the mitogenomes of sequenced grass species.

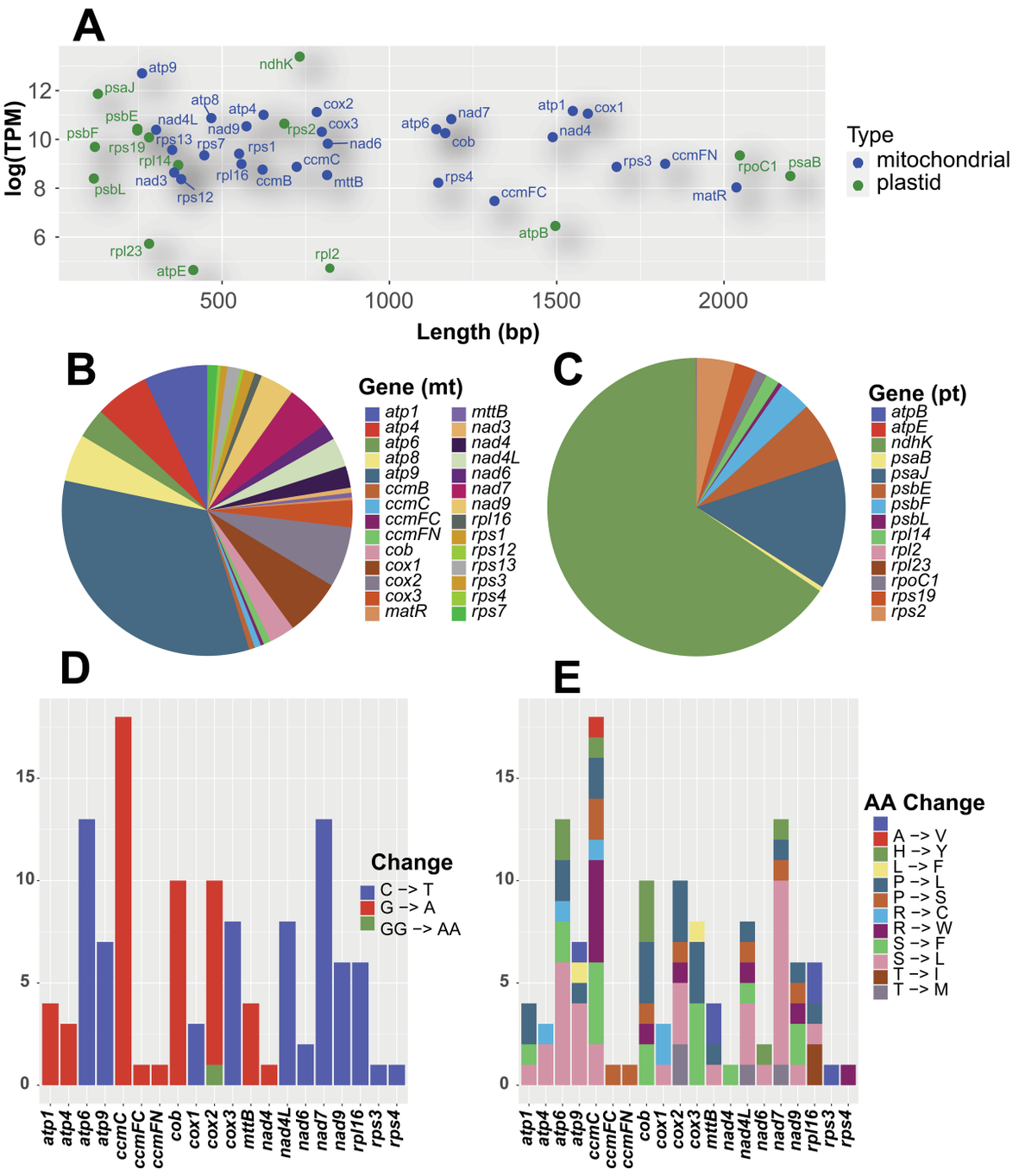


**Fig. 4** *A*, Location and relative levels of expression (transcripts per million [TPM]) for mitochondrial coding DNA sequences (CDS) and plastid-like sequences. *B*, Relative expression levels of mitochondrial CDS. *C*, Relative expression levels of plastid-like sequences. *D*, Numbers of putative RNA editing sites for each mitochondrial CDS (C → U on forward strand or G → A on reverse strand). *E*, Predicted amino acid changes at putative RNA editing sites per mitochondrial CDS.

transcripts were ATP synthase (*atp*; TPM range = 33,500.5–327,781.1; fig. 4*A*, 4*B*), followed by cytochrome c oxidase (*cox*; TPM range = 30,052.4–67,602.3) and NADH dehydrogenase (*nad*; TPM range = 5668.2–50,473.9; fig. 4*A*, 4*B*). Expression was also detected for plastid-like regions, predominantly *ndhK* (TPM = 654,340.2) and *psaJ* (142,073.1; fig. 4C). Together, these two regions accounted for >75% of all putatively expressed plastid-like regions, despite the former having multiple internal

stop codons and the latter being truncated at the 3′ end. There was evidence of C → U RNA editing among mitochondrial CDS as well, ranging from one site per gene to 18 sites per gene (viz. *ccmC*; fig. 4*D*). The vast majority of RNA editing involved replacement substitutions, with SER → LEU being the most common type (fig. 4*E*).

Searches for TE-like sequences recovered 29 hits in RepeatMasker, including sequences similar to class I retrotransposons ($n = 14$) and class II DNA transposons ($n = 10$; fig. S1). Class I retrotransposon-like sequences belonged to LTR/Copia ($n = 4$; length range = 102–646 bp), LTR/Gypsy ($n = 9$; 44–1313 bp), and LINE/L1 ($n = 1$; 108 bp) superfamilies. Among class II DNA transposon-like sequences, nine were similar to DNA/PIF-Harbinger (47–6881 bp), two of which were >6 kb in length (fig. S1). Another class II–like sequence corresponded to the DNA/CMC-EnSpm superfamily (139 bp). Five TE-like hits were unclassified, ranging from 32 to 2437 bp in length. Additional searches with HelitronScanner found three hits for Helitron-like sequences, of 571, 14,875, and 5477 bp. The first was identified in the spacer region between *rps12* and *ccmB*, the second between *nad4* and *nad1* intron 3, and the third overlapping with *cox1*. MiteFinderII found three hits of MITE-like sequences with lengths of 246, 400, and 285 bp. The first was identified between *trnS-GGA* and *rps7*, the second between *trnP-TGG* and *nad5* (exon 5), and the third between *ccmFC* and *trnK-TTT* (which is duplicated within the largest IR region). Taken together, 9.05% of the *M. vimineum* mitogenome is composed of TE-like sequences.

Analysis of the mitogenome assembly with Kraken2 supports a genome that is free from foreign sequences and contamination (fig. S2). Scanning of *k*-mers comprising 100-bp segments of the mitogenome against those found in genomes representing plants, bacteria, archaea, viruses, fungi, UniVec contaminants, and the human genome resulted in classification of 77.52% of *k*-mers, of which 77.45% were classified as characteristic of *k*-mers optimized to the node representing the hypothesized ancestor of Viridiplantae, 74.44% of Liliopsida, and 72.3% of Poaceae. The remaining unclassified *k*-mers represent either our incomplete knowledge of mitogenomic diversity or the presence of sequences unique to the mitogenome of this species.

### *Phylogenomic Analyses Using Mitochondrial CDS*

Analysis of 7019 aligned positions across 28 protein-coding mitochondrial genes (total gaps/missing data content = 7.2%, total parsimony-informative characters = 1955) under the GHOST heterotachy model yielded a tree topology with generally high bootstrap support (BS) values (lnL = −31,000.1643, BIC score = 65,013.6522, total branch/model free parameters = 137; fig. 5*A*).

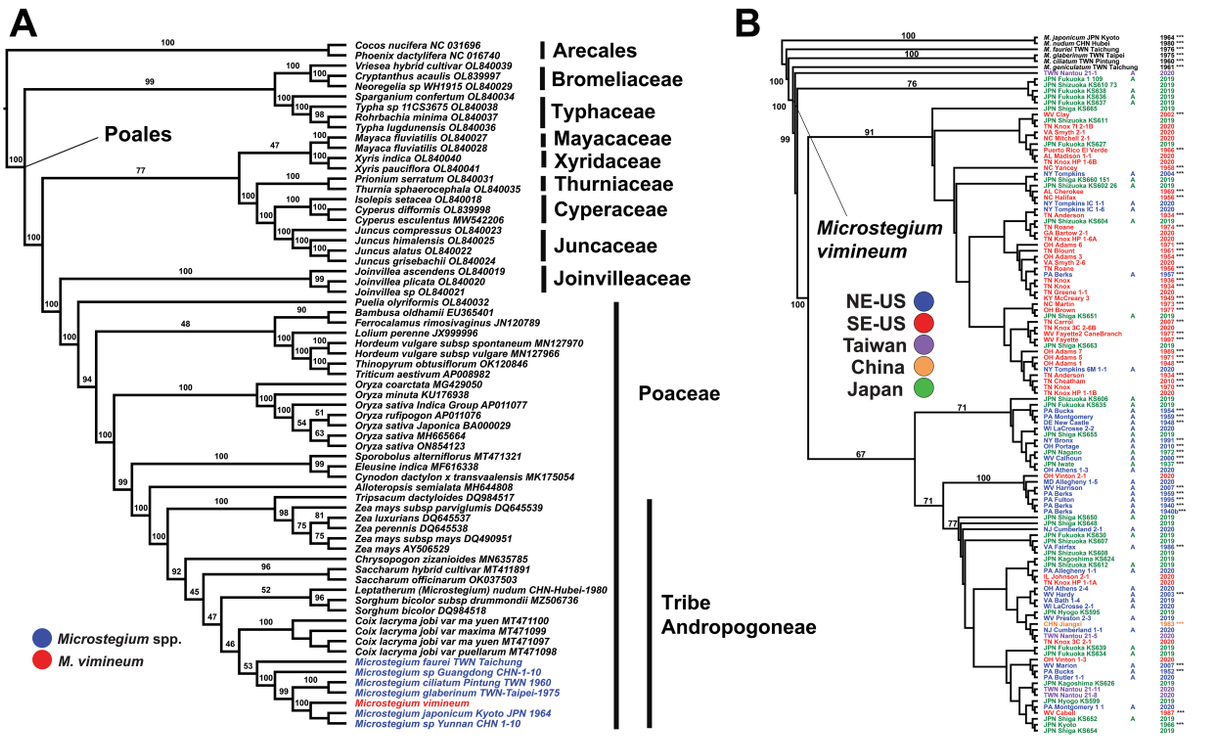


**Fig. 5** *A*, Maximum likelihood phylogenetic tree based on a 7019-bp alignment of mitochondrial coding DNA sequences (CDS) under the GHOST heterotachy model. Numbers above branches indicate bootstrap support. *Microstegium* species are in blue text, with *M. vimineum* in red. *B*, Maximum likelihood phylogenetic tree among mitochondrial haplotypes of *M. vimineum*. Colors indicate regions from which samples were collected: green = Japan; orange = China; purple = Taiwan; red = southeastern US; blue = northeastern US. A = the presence of awned florets (the lack thereof indicates a lack of awned florets). The numbers on the right list the year each sample was collected; all samples collected prior to 2019 came from herbarium specimens. Three asterisks indicate herbarium specimens.

Among the families of order Poales, mitochondrial data placed Typhaceae as sister to Bromeliaceae + the remainder of the order (BS = 99). In the latter clade, Xyridaceae were sister to a clade composed of ((Mayacaceae, (Thurniaceae, (Cyperaceae, Juncaceae))), (Joinvilleaceae, Poaceae)); all BS = 100 excluding the sister relationship of (*Mayaca, Xyris*; BS = 47) and Mayacaceae as sister of (Thurniaceae, Cyperaceae, Juncaceae; BS = 77). Within Poaceae, *Puelia* (Puelioideae) was supported as sister to the remaining taxa (BS = 100), followed by representatives of tribes Bambusoideae (*Bambusa*, *Ferrocalamus*) and Pooideae (e.g., *Lolium*, *Triticum*, *Thinopyrum*, *Hordeum*), but with a lack of support for the latter subfamilies as sister to one another (BS = 48). Following this, Oryzoideae (*Oryza*; BS = 100) was placed as sister to Chloridoideae (*Eleusine*; BS = 100) and Panicoideae (BS = 100). Within Panicoideae, *Alloteropsis* was sister to a clade comprising members of the subtribe Andropogoneae (BS = 99). Within Andropogoneae, (*Tripsacum*, *Zea*) were sister to a clade composed of *Sorghum*, *Microstegium*, *Saccharum*, *Chrysopogon*, and *Coix* (BS = 100), with BS = 92 for the latter. However, support was generally low within this clade. *Leptatherum* (*Microstegium*) *nudum* (Trin.) C.H. Chen, Kuoh, Chang Sen & Veldkamp was placed as sister to two accessions of *Sorghum*, but with no support (BS = 52). Sister to this clade is a clade of (*Coix, Microstegium*), but again, with no support (BS = 46). Among the remaining accessions of *Microstegium, M. faurei* (Havata) Honda was sister to the rest, but with no support (BS = 52), while *M. vimineum* was placed as sister to *M. japonicum* (Miq.) Koidz. and an unknown accession of *Microstegium* from Yunnan, China (BS = 100); the latter specimen was 100% identical to *M. japonicum*.

### *Assessment of Relationships among Mitochondrial Haplotypes of* M. vimineum

Analysis of genome skim datasets for 118 accessions from the US (invasive) and Asia (native) yielded 3913 mitochondrial variants. Phylogenetic analysis of the data in IQtree2 yielded a tree with two principal clades corresponding to samples from the invasive range (best-fit model = SYM + ASC + R5, lnL = −47,277.03, BIC score = 96,588.99, total branch/model free parameters = 246; fig. 5*B*). These two clades were sister to a clade of haplotypes from Japan (from Fukuoka, Shiga, and Shizuoka), collectively sister to a single haplotype from Nantou, Taiwan. The first clade containing accessions from the invasive range was primarily composed of individuals from the southeastern US that lack awns (BS = 91). Interspersed among these invasive-range accessions were several accessions from Japan. Bootstrap values among individual haplotypes within this clade were generally low. The second clade was composed primarily of awned forms from the northeastern US, but this clade as a whole received weak support (BS = 67). Invasive haplotypes in this clade were interspersed among those from Japan and Taiwan, with a single haplotype from China; likewise, support values were generally low within this clade. There were exceptions, however: four haplotypes from Tompkins County, New York, grouped with the predominantly southern clade (predominantly southern US awnless accessions), whereas six haplotypes from eastern Tennessee, southern West Virginia, southern Ohio, and southern Illinois grouped with the predominantly northern clade.

## Discussion

### *Organellar Genome Sequencing and Assembly*

We sequenced and analyzed the 478,010-bp mitochondrial genome of the invasive *Microstegium vimineum*, revealing a genome typical of previously sequenced grasses. Grass mitogenomes represented in NCBI GenBank range from 294 to 740 kb; thus, *M. vimineum* has a somewhat average genome size with gene content typical of other grasses. Overall, gene space occupies 13.2% of the genome, followed by TE-like sequence (9.05%) and plastid-like sequence (2.4%), leaving 75.3% as unknown.

### *Analyses of Repetitive DNA, Structural Variation, Plastid-Like DNA, RNA Editing, TEs, and Foreign-Acquired Sequences*

As observed in other mitogenomes, both large (i.e., >1000 bp) and small direct and indirect repeats are present in *M. vimineum* (figs. 1, 2). Further, these repeats are associated with putative isomeric variants, which argues against the existence of a master circle (figs. 1, 2; Sloan 2013). In fact, the genome could not be circularized with PacBio or Illumina reads, casting further doubt on the existence of a single circular structure. Insertions of plastid-like DNA regions, many of which are divergent from their homologs in the plastid genome of *M. vimineum*, suggest that many of these regions may be considered "ancient" transfers, while some others either may have occurred more recently or are the result of "copy correction" via gene conversion (fig. 3*A*; Sloan and Wu 2014). The total extent of plastid DNA content detected in the mitogenome species is not extreme (2.4% compared to >10% in the palm *Phoenix dactylifera*; Fang et al. 2012) but is similar to that in other grasses (e.g., Clifton et al. 2004). The apparent expression of some of these regions presents a conundrum, as our evidence suggests that these are nonfunctional, lacking intact open reading frames. One possible explanation would be that these plastid-like regions lie within expressed cistrons and thus are transcribed but potentially spliced out or their RNAs modified after transcription (Cardi et al. 2012). Previous research has shown that most of the mitogenome can be transcribed, and that extensive posttranscriptional modification produces the mature transcripts (Holec et al. 2006; Ruwe et al. 2016). RNA editing was also observed within CDS of *M. vimineum*, a common feature of both organellar genomes in plants; this process is likely essential for proper gene expression and further may preserve the integrity of secondary structure in organellar genomes (e.g., Maier et al. 1996). It should be noted that only a single tissue type (young developing leaf tissue) from a single individual was included here, and thus the need remains for gene expression studies across tissue types, developmental stages, and environmental conditions to explore the transcriptional landscape in this invasive species.

Integration of nuclear-derived TE-like sequences provides a partial explanation for plant mitochondrial genome size expansion (Marienfeld et al. 1999; Mower et al. 2012; Zhao et al. 2018). Previous research on *Arabidopsis thaliana* (L.) Heynh., *Citrullus lanatus* (Thunb.) Matsum. & Nakai, *Cucurbita pepo* L., *Ligustrum quihoui* Carrière, and *Elymus sibiricus* L. has reported that ≈1%–6% of their respective mitogenomes are nuclear-derived TE-like sequences (Knoop et al. 1996; Alverson et al. 2010; Yu et al. 2020; Xiong et al. 2022). Although

9.05% of the mitogenome of *M. vimineum* is occupied by similar TE-like sequences (fig. S1), the majority of these duplicated sequences are fragmentary. These results indicate frequent and independent DNA transfers from nuclear to mitochondrial genome and that the fragmented copies could have been generated from former complete sequences that later became degraded, that they originated from incomplete transposition events, or that they were scrambled by intramolecular recombination—frequent in plant mitogenomes (Knoop et al. 1996; Notsu et al. 2002). Regardless, the landscape of TE-like sequences in plant mitogenomes is not well explored.

An absence of sequence from distantly related plant lineages, or other lineages in general, suggests that the mitogenome of *M. vimineum* is free of foreign sequence, that foreign sequence is too recombined to identify, or that *k*-mers present are highly unique and are not contained in the genomes included in our analyses (fig. S2). We find the latter two explanations unlikely, given the broad range of lineages represented in our Kraken2 databases. Additionally, none of the *k*-mers from our assembly were classified when searched against the Eukaryotic Pathogen, Vector and Host Informatics Resource Database. Taken together, these results characterize a mitogenomic assembly that is free of confounding artifactual contamination resulting from interactions in the lab or during necessary bioinformatic components of our work.

### *Phylogenomic Analyses Using Mitochondrial CDS*

*Microstegium* species, including *M. vimineum*, are clearly placed within the grass tribe Andropogoneae based on mitochondrial data (fig. 5*A*). Our analysis of mitochondrial coding regions suggests a close relationship among most of the *Microstegium* species sampled here, with the exclusion of *Leptathera nudum* (formerly placed in *Microstegium*) and possibly *M. faurei*; the latter was placed as sister of *M. ciliatum* (Trin.) A. Camus, *M. glaberrimum* (Honda) Koidz, *M. japonicum*, and *M. vimineum*, but with no support. This is in contrast to other studies based on plastid DNA in which species of *Microstegium* occupy different clades within the Andropogoneae, though the level of *Microstegium* spp. sampling in those studies and the lack of available mitogenomes across Andropogoneae in the current study are insufficient for confident placement of the different species. Lloyd Evans et al. (2019) placed *M. vimineum* with moderate support as sister to *Polytrias* Hack. and two species of *Sorghastrum* Nash, all of which are sister to a clade composed of *Miscanthus* Andersson and *Saccharum* spp. based on five low-copy nuclear genes. In that study, *M. vimineum* is estimated to have diverged from a common ancestor with *Polytrias* and *Sorghastrum* between 7 and 10.5 million years ago, but sampling included only *M. vimineum* from the genus *Microstegium*. Data from complete plastid genomes placed *M. vimineum* as sister to two genera: *Kerriochloa*, with a single species *Kerriochloa siamensis* C. E. Hubb (Thailand, Vietnam), and *Sehima* Forssk., comprising five species from Africa, Asia, and Australia (Welker et al. 2020). But again, *M. vimineum* was the only representative of *Microstegium* sampled.

Chen et al. (2009, 2012) conducted a phylogenetic analysis and taxonomic treatment of *Microstegium* based on nuclear internal transcribed spacer sequencing and morphology. Our findings of *L. nudum* as sister of *Sorghum*, with other species of *Microstegium* occupying a different clade (more closely allied with *Coix*) are generally in agreement with these previous studies, but with some key differences. First, Chen et al. (2012) identify two clades, a *nudum* clade (*japonicum*, *nudum*, *somae* (Hayata) Ohwi) and a *vimineum* clade (*ciliatum, faurei, geniculatum, vimineum*). In our phylogenetic analysis, only *L. nudum* (formerly included in *Microstegium*) grouped outside the main clade of *Microstegium*, but support overall for the latter is weak (fig. 5*A*). Further, *M. vimineum* was strongly supported as sister to *M. japonicum* and an unknown species of *Microstegium* (BS = 100), whereas the analysis of Chen et al. (2012) placed *M. vimineum* as sister to *M. ciliatum*, but with low support (BS = 69). The placement of *L. nudum*, while not strongly supported, does lend some credibility to the decision to recognize this species as a member of a separate genus outside of *Microstegium*. Though the taxon sampling of mitogenomes in the current study is not comprehensive, it does represent the largest amount of data analyzed to date on the taxonomic status of the genus.

Based on our analysis and previous studies, it is indeed possible that *Microstegium* is polyphyletic, perhaps reflecting a complex, reticulate history of allopolyploidy that is broadly observed among the Andropogoneae (e.g., Estep et al. 2014; Hawkins et al. 2015; Arthan et al. 2017; Ramachandran et al. 2021). *Microstegium vimineum* is a known polyploid, with $2n = 20$ chromosomes, twice that of the base number of $2n = 10$ in Andropogoneae (Watson and Dallwitz 1992). Further, analysis of the recently published chromosome-level nuclear genome of *M. vimineum* revealed strong evidence of a paleopolyploidy event, with about one-third of all nuclear genes present as duplicate copies (Ramachandran et al. 2021). Further, comparative analysis of terminal repeats of TEs throughout the nuclear genome, calibrated to a grass-specific TE divergence rate (Ma and Bennetzen 2004), revealed a burst of TE activity roughly 1–2 million years ago, possibly coinciding with genomic shock associated with a polyploidy event (Ramachandran et al. 2021). This warrants further study with dense taxon sampling across the tribe, including multiple species and accessions of *Microstegium*, and employing genome-wide plastid, mitochondrial, and nuclear markers to test hypotheses of allopolyploid origins within the currently circumscribed *Microstegium* and other genera.

### *Assessment of Relationships among Mitochondrial Haplotypes of* M. vimineum

Patterns of mitogenomic SNP variation within *M. vimineum* reveal a complex invasion history (fig. 5*B*). The finding of a predominantly northern awned clade and a southern awnless clade mirrors that based on nuclear SNP data (Barrett et al. 2022) and plastid data (C. W. Corbett et al., unpublished data). Further, there is evidence of multiple invasions and subsequent establishments from the native range, with a likely initial successful awnless invasion in the southeastern US and at least one more successful invasion in the northeastern US of the awned form, likely in eastern Pennsylvania. Because this species was used as packing for shipments from Asia, it is plausible for multiple invasions to have occurred, perhaps bearing higher than expected genetic diversity (i.e., contrasted with expectations of a severe genetic bottleneck upon a single invasion) if seeds from multiple plants continually became established (e.g., Sakai et al. 2001; Kolbe et al. 2004; Frankham 2005; Dlugosch and Parker 2008; Sutherland et al. 2021). Further, there is evidence that each putative

invasion and subsequent spread led to long-distance dispersal within the invasive range over the last century, with southern mitotypes present as far north as central-western New York State (i.e., Tompkins County, New York) and northern mitotypes present as far south as eastern Tennessee (fig. 5*B*). Indeed, samples collected in 2020 from the original site where stiltgrass was collected 101 years before (Knox County, Tennessee) revealed a mix of northern and southern mitotypes, suggesting that this species has been dispersed extensively over the past few decades via anthropogenic activity. This is significant, as such long-distance dispersal may lead to rapid admixture of previously separated genotypes from the native range, allowing the genomic potential for rapid adaptation to local conditions (Verhoeven et al. 2010; Rius and Darling 2014) and thus presenting a mechanism for increased invasive potential over time (Dlugosch and Parker 2008; Keller and Taylor 2010; Dlugosch et al. 2015; Sutherland et al. 2021).

There is evidence that *M. vimineum* has experienced rapid adaptation after becoming established in the invasive range, in terms of flowering phenology across a latitudinal gradient, and growth/reproductive advantages of invasive populations compared with those in the native range, in line with the evolution of increased competitive ability hypothesis (Flory et al. 2011; Novy et al. 2013; Huebner et al. 2022). Barrett et al. (2022) suggested that this may further extend to selection in the invasive range for different awn phenotypes. In the eastern US, there is a strong latitudinal pattern of awnless forms in the South, long-awned forms in the North, and intermediate- or short-awned forms at midlatitudes. A similar but relatively weaker pattern was observed in Asia, with both awned and awnless phenotypes intermixed at low- and midlatitudes but a predominance of awned forms at higher latitudes. Awns are hypothesized to aid in microsite dispersal and burial via hygroscopic movement, effectively drilling the seed-containing floret into the seed bank (Cavanagh et al. 2020). Awns are expected to play a role in seedling burial and increased survival from frequent and intense soil freezing events at higher latitudes. Our mitochondrial SNP analysis (fig. 5*B*) and previous analysis of nuclear SNP variation (Barrett et al. 2022) support a scenario consistent with intensified, post-invasion selection for awn phenotypes in the eastern US, favoring awnless forms at lower latitudes and awned forms at higher latitudes. Habitat filtering may have also played a role (Weiher and Keddy 1995) by selecting which phenotypes were successful in their initial invasions, with a higher likelihood of successful invasion hypothesized in the South by awnless forms and in the North by awned forms. We are currently conducting burial, germination, and seed survival experiments to test hypotheses on selection for awns and associated phenotypes in the invasive range.

Genome sequencing efforts in invasive plant species are in their infancy but hold great potential for the identification, phylogenetic placement, evolutionary ecology, and management of these species. High-quality genome sequences and annotations provide much-needed baseline data, enabling subsequent studies of invasion routes, invasion history, and other diverse applications in invasion biology. Here we have sequenced a reference mitogenome for *M. vimineum*, one of the most invasive plants in eastern North America, to aid in such future studies. While characterizing genome structure and content, we also corroborated recent studies on the complex invasion history and spatiotemporal patterns of mitogenomic variation in the native and invasive ranges. Most importantly, such genomic resources will aid in efforts to predict ongoing patterns of spread within this species and responses to climate change and possibly help predict future threats from other invasive species, allowing genomics-informed forecasting.

## Acknowledgments

This work was supported by the US National Science Foundation (award OIA-1920858), the West Virginia University (WVU) Department of Biology, and the USDA Forest Service Northern Research Station. We thank Mark Daly, Jasmine Haimovitz, Joanna Gallagher, and Jordan Zhang at Dovetail Genomics (Cantata Bio) for expert assistance with long-read sequencing and GeneWiz for RNA sequencing. We thank J. Beck, M. Latvis, N. Kooyers, M. McKain, E. Sigel, and B. Sutherland for feedback and discussion. We thank the following collaborators for providing contemporary field-collected material: M. McKain, G. Matlack, G. Moore, S. Kuebbing, B. Molano-Flores, A. Kennedy, J. Fagan, N. Koenig, P. Crim, G. Scott, B. Foster, M. Heberling, A. Bowe, P. Wolf, K. Willard, and J. McNeal. For access to herbarium collections we thank Tiana Rehman (BRIT), Bonnie Isaac (CM), Mason Heberling (CM), John Freudenstein (OS), Anna Statler (BH), Tanya Livshultz (PH), Meghann Toner (US), Lauren Boyle (MO), Margaret Oliver (TENN), and Donna Ford-Werntz (WVA). For assistance with genomic sequencing, we thank R. Percifield, D. Primerano, and J. Fan. For collections in Japan, we thank C. Hara, S. Mori, M. Sato, T. Shimizu, and K. Tanaka. We thank the WVU Genomics Core Facility for support provided to help make this publication possible and for CTSI grant U54 GM104942, which in turn provides financial support to the WVU Core Facility. We further acknowledge WV-INBRE (P20GM103434), a COBRE ACCORD grant (1P20GM121299), and a West Virginia Clinical and Translational Science Institute grant (2U54GM104942) in supporting the Marshall University Genomics Core (research citation: Marshall University Genomics Core Facility, RRID:SCR_018885). C. F. Barrett conceived the study, analyzed data, and led the writing of the manuscript. K. Suetsugu, W.-B. Yu, and C.-H. Chen provided Asian samples and contributed to drafts of the manuscript. D. Ramachandran and B. T. Sinn analyzed data and helped draft the manuscript. C. D. Huebner collected samples, maintained plants in a controlled environment (growth chamber), and helped draft the manuscript. C. W. Corbett generated data, assisted with data analyses, and helped draft the manuscript. All authors have reviewed and approved the final manuscript.

## Appendix

Voucher information: species, accession, US county (if applicable), region/state, country, herbarium code, collector, collection number. Herbarium codes: BH (Bailey Hortorium Herbarium), BRIT (Botanical Research Institute of Texas), CM (Carnegie Museum of Natural History), MO (Missouri Botanical Garden), OS (Ohio State University Herbarium), PH (Academy of Natural Sciences), TENN (University of Tennessee Herbarium), WVA (West Virginia University Herbarium).

*Leptatherum nudum* (Trin.) C.H. Chen, Kuoh, Chang Sen & Veldkamp, M-nudum-CHN-Hubei-1980-83-S44, n/a, Hubei, China, 1980, CM, Bartholomew et al., s.n.; *Microstegium vimineum* (Trin.) A. Camus, CHN-Jiangxi-1983-12-S7, n/a, Jiangxi, China, 1983, CM, Yao, 8711; *Microstegium vimineum* (Trin.) A. Camus, 111-JPN-Fukuoka-KS630-S9, n/a, Fukuoka, Japan, 2019, WVA, Suetsugu, 630; *Microstegium vimineum* (Trin.) A. Camus, 115-JPN-Fukuoka-KS636-S11, n/a, Fukuoka, Japan, 2019, WVA, Suetsugu, 636; *Microstegium vimineum* (Trin.) A. Camus, 116-JPN-Fukuoka-KS637-S12, n/a, Fukuoka, Japan, 2019, WVA, Suetsugu, 637; *Microstegium vimineum* (Trin.) A. Camus, 117-JPN-Fukuoka-KS638-S13, n/a, Fukuoka, Japan, 2019, WVA, Suetsugu, 638; *Microstegium vimineum* (Trin.) A. Camus, 118-JPN-Fukuoka-KS639-S14, n/a, Fukuoka, Japan, 2019, WVA, Suetsugu, 639; *Microstegium vimineum* (Trin.) A. Camus, JPN-Fukuoka-1-109-S58, n/a, Fukuoka, Japan, 2019, WVA, Suetsugu, 633; *Microstegium vimineum* (Trin.) A. Camus, JPN-Fukuoka-KS627-30-S17, n/a, Fukuoka, Japan, 2019, WVA, Suetsugu, 627; *Microstegium vimineum* (Trin.) A. Camus, JPN-Fukuoka-KS634-31-S18, n/a, Fukuoka, Japan, 2019, WVA, Suetsugu, 634; *Microstegium vimineum* (Trin.) A. Camus, JPN-Fukuoka-KS635-32-S19, n/a, Fukuoka, Japan, 2019, WVA, Suetsugu, 635; *Microstegium vimineum* (Trin.) A. Camus, JPN-Shizuoka-KS604-67-S28, n/a, Fukuoka, Japan, 2019, WVA, Suetsugu, 604; *Microstegium vimineum* (Trin.) A. Camus, JPN-Hyogo-KS595-24-S11, n/a, Hyogo, Japan, 2019, WVA, Suetsugu, 595; *Microstegium vimineum* (Trin.) A. Camus, JPN-Hyogo-KS599-25-S12, n/a, Hyogo, Japan, 2019, WVA, Suetsugu, 599; *Microstegium vimineum* (Trin.) A. Camus, JPN-Kagoshima-KS624-28-S15, n/a, Kagoshima, Japan, 2019, WVA, Suetsugu, 624; *Microstegium vimineum* (Trin.) A. Camus, JPN-Kagoshima-KS626-29-S16, n/a, Kagoshima, Japan, 2019, WVA, Suetsugu, 626; *Microstegium japonicum* (Miq.) Koidz., M-japonicum-JPN-Kyoto-1964-84-S45, n/a, Kansai, Japan, 1964, CM, Murata, 19181; *Microstegium vimineum* (Trin.) A. Camus, JPN-Kyoto-1966-11-S6, n/a, Kansai, Japan, 1966, CM, Murata, G., 19905; *Microstegium vimineum* (Trin.) A. Camus, 92-JPN-Nagano-1972-S4, n/a, Nagano, Japan, 1972, CM, Shimizu, T., 24216; *Microstegium vimineum* (Trin.) A. Camus, 120-JPN-Shiga-KS648-S16, n/a, Shiga, Japan, 2019, WVA, Suetsugu, 648; *Microstegium vimineum* (Trin.) A. Camus, JPN-Shiga-KS650-122-S61, n/a, Shiga, Japan, 2019, WVA, Suetsugu, 650; *Microstegium vimineum* (Trin.) A. Camus, JPN-Shiga-KS651-123-S62, n/a, Shiga, Japan, 2019, WVA, Suetsugu, 651; *Microstegium vimineum* (Trin.) A. Camus, JPN-Shiga-KS652-124-S63, n/a, Shiga, Japan, 2019, WVA, Suetsugu, 652; *Microstegium vimineum* (Trin.) A. Camus, JPN-Shiga-KS654-126-S65, n/a, Shiga, Japan, 2019, WVA, Suetsugu, 654; *Microstegium vimineum* (Trin.) A. Camus, JPN-Shiga-KS655-127-S66, n/a, Shiga, Japan, 2019, WVA, Suetsugu, 655; *Microstegium vimineum* (Trin.) A. Camus, JPN-Shiga-KS660-151-S76, n/a, Shiga, Japan, 2019, WVA, Suetsugu, 660; *Microstegium vimineum* (Trin.) A. Camus, JPN-Shiga-KS663-154-S79, n/a, Shiga, Japan, 2019, WVA, Suetsugu, 663; *Microstegium vimineum* (Trin.) A. Camus, JPN-Shiga-KS665-156-S81, n/a, Shiga, Japan, 2019, WVA, Suetsugu, 665; *Microstegium vimineum* (Trin.) A. Camus, JPN-Shizuoka-KS602-26-S13, n/a, Shizuoka, Japan, 2019, WVA, Suetsugu, 602; *Microstegium vimineum* (Trin.) A. Camus, JPN-Shizuoka-KS606-69-S30, n/a, Shizuoka, Japan, 2019, WVA, Suetsugu, 606; *Microstegium vimineum* (Trin.) A. Camus, JPN-Shizuoka-KS607-70-S31, n/a, Shizuoka, Japan, 2019, WVA, Suetsugu, 607; *Microstegium vimineum* (Trin.) A. Camus, JPN-Shizuoka-KS608-71-S32, n/a, Shizuoka, Japan, 2019, WVA, Suetsugu, 608; *Microstegium vimineum* (Trin.) A. Camus, JPN-Shizuoka-KS610-73-S34, n/a, Shizuoka, Japan, 2019, WVA, Suetsugu, 610; *Microstegium vimineum* (Trin.) A. Camus, JPN-Shizuoka-KS611-74-S35, n/a, Shizuoka, Japan, 2019, WVA, Suetsugu, 611; *Microstegium vimineum* (Trin.) A. Camus, JPN-Shizuoka-KS612-27-S14, n/a, Shizuoka, Japan, 2019, WVA, Suetsugu, 612; *Microstegium vimineum* (Trin.) A. Camus, JPN-Iwate-1937-82-S43, n/a, Tohoku, Japan, 1937, CM, Iwabuchi, H., 5516; *Microstegium vimineum* (Trin.) A. Camus, TWN-N-21-11-S38, n/a, Nantou, Taiwan, 2020, WVA, Chen, TWN-N-21-11; *Microstegium vimineum* (Trin.) A. Camus, TWN-N-21-2-S29, n/a, Nantou, Taiwan, 2020, WVA, Chen, TWN-N-21-2; *Microstegium vimineum* (Trin.) A. Camus, TWN-N-21-5-S32, n/a, Nantou, Taiwan, 2020, WVA, Chen, TWN-N-21-5; *Microstegium vimineum* (Trin.) A. Camus, TWN-N-21-8-S35, n/a, Nantou, Taiwan, 2020, WVA, Chen, TWN-N-21-8; *Microstegium ciliatum* (Trin.) A. Camus, M-ciliatum-TWN-Pintung-1960-88-S49, n/a, Pintung, Taiwan, 2020, CM, Hsu, 1073; *Microstegium fauriei* (Hayata) Honda), M-fauriei-TWN-Taichung-1976-87-S48, n/a, Taichung, Taiwan, 2020, CM, Kuo, 7116; *Microstegium geniculatum* (Hayata) Honda, M-geniculatum-TWN-Taichung-1961-86-S47, n/a, Taichung, Taiwan, 2020, CM, Feung, 4439; *Microstegium glaberrimum* (Honda) Koidz., M-glaberinum-TWN-Taipei-1975-85-S46, n/a, Taipei, Taiwan, 2020, CM, Kuo, 6424; *Microstegium vimineum* (Trin.) A. Camus, AL-Cherokee-1969-S67, Cherokee, Alabama, USA, 2020, TENN, Kral, 37767; *Microstegium vimineum* (Trin.) A. Camus, AL-MAD-1-1-S51, Madison, Alabama, USA, 2020, WVA, Wolf, AL-MAD-1-1; *Microstegium vimineum* (Trin.) A. Camus, DE-New-Castle-1948-138-S68, New Castle, Delaware, USA, 1948, CM, Long, B., 68410; *Microstegium vimineum* (Trin.) A. Camus, GA-BAR-2-1-S55, Bartow, Georgia, USA, 2020, WVA, McNeal, GA-BAR-2-1; *Microstegium vimineum* (Trin.) A. Camus, IL-JOHN-2-1-S15, Johnson, Illinois, USA, 2020, WVA, Molano-Flores, IL-JOHN-2-1; *Microstegium vimineum* (Trin.) A. Camus, KY-McCreary3-1949-23-S10, McCreary, Kentucky, USA, 1949, MO, Reed, 16339; *Microstegium vimineum* (Trin.) A. Camus, 215-MD-GR-1-5-S15, Alleghany, Maryland, USA, 2019, WVA, Huebner, MD-GR-1-5; *Microstegium vimineum* (Trin.) A. Camus, NJ-CUMB-1-1-S5, Cumberland, New Jersey, USA, 2020, WVA, Moore, NJ-CUMB-1-1; *Microstegium vimineum* (Trin.) A. Camus, NJ-CUMB-2-2-S6, Cumberland, New Jersey, USA, 2020, WVA, Moore, NJ-CUMB-2-2; *Microstegium vimineum* (Trin.) A. Camus, NY-Bronx-1991-140-S69, Bronx, New York, USA, 1991, CM, Nee, M., 41826; *Microstegium vimineum* (Trin.) A. Camus, NY-Thomkins-2004-S86, Tompkins, New York, USA, 2004, BH, , ; *Microstegium vimineum* (Trin.) A. Camus, NY-TOM-6M-1-1-S20, Tompkins, New York, USA, 2020, WVA, Bowe, NY-TOM-6M-101; *Microstegium vimineum* (Trin.) A. Camus, NY-TOM-IC-1-1-S18, Tompkins, New York, USA, 2020, WVA, Bowe, NY-TOM-IC-1-1; *Microstegium vimineum* (Trin.) A. Camus, NY-TOM-IC-1-6-S19, Tompkins, New York, USA, 2020, WVA, Bowe, NY-TOM-IC-1-6; *Microstegium vimineum* (Trin.) A. Camus, NC-Halifax-1956-50-S21, Halifax, North Carolina, USA, 1956, BRIT, Ahles, 20724; *Microstegium vimineum* (Trin.) A. Camus, NC-Yancey-1958-51-S22, Yancey, North

Carolina, USA, 1958, BRIT, Ahles, 50776; *Microstegium vimineum* (Trin.) A. Camus, NC-Martin-1973-76-S37, Martin, North Carolina, USA, 1973, CM, Boufford, D.E., 12249; *Microstegium vimineum* (Trin.) A. Camus, NC-SP-2-1-S57, Mitchell, North Carolina, USA, 2020, WVA, Barrett, NC-SP-2-1; *Microstegium vimineum* (Trin.) A. Camus, OH-Adams-Co1-1948-4-S4, Adams, Ohio, USA, 1948, OS, Barley, F., s.n.; *Microstegium vimineum* (Trin.) A. Camus, OH-Adams-Co3-1954-5-S5, Adams, Ohio, USA, 1954, OS, Barley, F., s.n.; *Microstegium vimineum* (Trin.) A. Camus, OH-Adams-Co5-1971-1-S1, Adams, Ohio, USA, 1971, OS, Barley, F., s.n.; *Microstegium vimineum* (Trin.) A. Camus, OH-Adams-Co6-1971-2-S2, Adams, Ohio, USA, 1971, OS, Barley, F., s.n.; *Microstegium vimineum* (Trin.) A. Camus, 89-Brown-OH-1977-S1, Brown, Ohio, USA, 1977, OS, Cusick, A.W., s.n.; *Microstegium vimineum* (Trin.) A. Camus, OH-Adams-Co7-1989-3-S3, Adams, Ohio, USA, 1989, OS, Barley, F., s.n.; *Microstegium vimineum* (Trin.) A. Camus, 91-Portage-OH-2010-S3, Portange, Ohio, USA, 2010, OS, Gardner, R.L., 6970; *Microstegium vimineum* (Trin.) A. Camus, OH-ATH-1-3-S1, Athens, Ohio, USA, 2020, WVA, Matlack, OH-ATH-1-3; *Microstegium vimineum* (Trin.) A. Camus, OH-ATH-2-4-S2, Athens, Ohio, USA, 2020, WVA, Matlack, OH-ATH-2-4; *Microstegium vimineum* (Trin.) A. Camus, OH-VIN-1-3-S12, Vinton, Ohio, USA, 2020, WVA, Scott, OH-VIN-1-3; *Microstegium vimineum* (Trin.) A. Camus, OH-VIN-2-1-S13, Vinton, Ohio, USA, 2020, WVA, Scott, OH-VIN-2-1; *Microstegium vimineum* (Trin.) A. Camus, PA-Berks-1940-233a-S37, Berks, Pennsylvania, USA, 1940, PH, Brumbach, 3277; *Microstegium vimineum* (Trin.) A. Camus, PA-Berks-1940-75-S36, Berks, Pennsylvania, USA, 1940, PH, Wilkens, 6471; *Microstegium vimineum* (Trin.) A. Camus, Bucks-1952-George-S45, Bucks, Pennsylvania, USA, 1952, PH, Long, 75812; *Microstegium vimineum* (Trin.) A. Camus, PA-Bucks-1954-26-S48, Bucks, Pennsylvania, USA, 1954, PH, Wherry, sn; *Microstegium vimineum* (Trin.) A. Camus, PA-Berks-1957b-S41, Berks, Pennsylvania, USA, 1957, PH, Wilkens, 9182; *Microstegium vimineum* (Trin.) A. Camus, PA-Berks-1959-S43, Berks, Pennsylvania, USA, 1959, PH, Berkheimer, 19765; *Microstegium vimineum* (Trin.) A. Camus, PA-Montgomery-1959-S42, Montgomery, Pennsylvania, USA, 1959, PH, Wherry, sn; *Microstegium vimineum* (Trin.) A. Camus, PA-Fulton-1995-79-S40, Fulton, Pennsylvania, USA, 1995, CM, Grund, 1392; *Microstegium vimineum* (Trin.) A. Camus, PA-ALLE-1-1-S7, Allegheny, Pennsylvania, USA, 2020, WVA, Kuebbing, PA-ALLE-1-1; *Microstegium vimineum* (Trin.) A. Camus, PA-BUT-1-1-S16, Butler, Pennsylvania, USA, 2020, WVA, Heberling, PA-BUT-1-1; *Microstegium vimineum* (Trin.) A. Camus, PA-MONT-1-1-S3, Montgomery, Pennsylvania, USA, 2020, WVA, Moore, PA-MONT-1-1; *Microstegium vimineum* (Trin.) A. Camus, PR-ElVerdeExSta-1966-52-S23, Rio Grande, Puerto Rico, USA, 1966, BRIT, Duncan, sn; *Microstegium vimineum* (Trin.) A. Camus, TN-Anderson-1934-53-S24, Anderson, Tennessee, USA, 1934, TENN, Jennison, 4360; *Microstegium vimineum* (Trin.) A. Camus, TN-Anderson-1934-S61, Anderson, Tennessee, USA, 1934, BRIT, Jennison, 3348; *Microstegium vimineum* (Trin.) A. Camus, TN-Knox-1934-S65, Knox, Tennessee, USA, 1934, TENN, Miller, 3482; *Microstegium vimineum* (Trin.) A. Camus, TN-Knox-1936-16-S9, Knox, Tennessee, USA, 1936, MO, Jennison, 260; *Microstegium vimineum* (Trin.) A. Camus, TN-Roane-1956-S66, Roane, Tennessee, USA, 1956, TENN, Norris & DeSelm, 21779; *Microstegium vimineum* (Trin.) A. Camus, TN-Bount-1961-S62, Blount, Tennessee, USA, 1961, TENN, Pringle, 29862; *Microstegium vimineum* (Trin.) A. Camus, TN-Knox-1970-S74, Knox, Tennessee, USA, 1970, TENN, Somers & Bowers, 81; *Microstegium vimineum* (Trin.) A. Camus, TN-Roane-1974-80-S41, Roane, Tennessee, USA, 1974, CM, Hedge, 50096; *Microstegium vimineum* (Trin.) A. Camus, TN-Carrol-2007-S71, Carrol, Tennessee, USA, 2007, TENN, Crabtree & McCoy, sn; *Microstegium vimineum* (Trin.) A. Camus, TN-Cheatham-2010-S68, Cheatham, Tennessee, USA, 2010, TENN, Klagstad, 432; *Microstegium vimineum* (Trin.) A. Camus, TN-KNO-3C-2-1-S22, Knox, Tennessee, USA, 2020, WVA, Barrett, TN-KNO-3C-2-1-S22; *Microstegium vimineum* (Trin.) A. Camus, TN-KNO-3C-2-6-B-S44, Knox, Tennessee, USA, 2020, WVA, Barrett, TN-KNO-3C-2-6-B-S44; *Microstegium vimineum* (Trin.) A. Camus, TN-KNO-7I-2-1-B-S47, Knox, Tennessee, USA, 2020, WVA, Barrett, TN-KNO-7I-2-1-B-S47; *Microstegium vimineum* (Trin.) A. Camus, TN-KNO-HP-1-1-A-S24, Knox, Tennessee, USA, 2020, WVA, Barrett, TN-KNO-HP-1-1-A-S24; *Microstegium vimineum* (Trin.) A. Camus, TN-KNO-HP-1-1-B-S45, Knox, Tennessee, USA, 2020, WVA, Barrett, TN-KNO-HP-1-1-B-S45; *Microstegium vimineum* (Trin.) A. Camus, TN-KNO-HP-1-6-A-S25, Knox, Tennessee, USA, 2020, WVA, Barrett, TN-KNO-HP-1-6-A-S25; *Microstegium vimineum* (Trin.) A. Camus, TN-KNO-HP-1-6-B-S46, Knox, Tennessee, USA, 2020, WVA, Barrett, TN-KNO-HP-1-6-B-S46; *Microstegium vimineum* (Trin.) A. Camus, TN-LPG-1-1-S59, Greene, Tennessee, USA, 2020, WVA, Barrett, TN-LPG-1-1-S59; *Microstegium vimineum* (Trin.) A. Camus, VA-Fairfax-1986-S80, Fairfax, Virginia, USA, 1986, TENN, Fosberg, 65307; *Microstegium vimineum* (Trin.) A. Camus, 206-VA-Bath-1-4-S8, Bath, Virginia, USA, 2019, WVA, Barrett, VA-BATH-1-4; *Microstegium vimineum* (Trin.) A. Camus, VA-SG-2-1-S49, Smyth, Virginia, USA, 2020, WVA, Barrett, VA-SMYTH-2-1; *Microstegium vimineum* (Trin.) A. Camus, VA-SG-2-6-S50, Smyth, Virginia, USA, 2020, WVA, Barrett, VA-SMYTH-2-6; *Microstegium vimineum* (Trin.) A. Camus, WV-Fayette-1977-105-S54, Fayette, West Virginia, USA, 1977, WVA, Grafton, sn; *Microstegium vimineum* (Trin.) A. Camus, 104-Cabell-Boone-WV-1987-S7, Cabell, West Virginia, USA, 1987, WVA, Cusick, 27164; *Microstegium vimineum* (Trin.) A. Camus, WV-Fayette-1997-103-S53, Fayette, West Virginia, USA, 1997, WVA, Grafton, sn; *Microstegium vimineum* (Trin.) A. Camus, WV-Calhoun-2000-96-S52, Calhoun, West Virginia, USA, 2000, WVA, Grafton, sn; *Microstegium vimineum* (Trin.) A. Camus, 99-WV-Clay-2002-S6, Clay, West Virginia, USA, 2002, WVA, Grafton, sn; *Microstegium vimineum* (Trin.) A. Camus, WV-Hardy-2003-107-S56, Hardy, West Virginia, USA, 2003, WVA, Grafton, sn; *Microstegium vimineum* (Trin.) A. Camus, WV-Harrison-2007-106-S55, Harrison, West Virginia, USA, 2007, WVA, Grafton, sn; *Microstegium vimineum* (Trin.) A. Camus, WV-Marion-2007-145-S74, Marion, West Virginia, USA, 2007, WVA, Grafton, sn; *Microstegium vimineum* (Trin.) A. Camus, WV-SR-2-3-225-S85, Preston, West Virginia, USA, 2019, WVA, Huebner & Barrett, WV-SR-2-1; *Microstegium vimineum* (Trin.) A. Camus, WI-LAC-2-1-S8, LaCrosse, Wisconsin, USA, 2020, WVA, Molano-Flores, WI-LAC-2-1; *Microstegium vimineum* (Trin.) A. Camus, WI-LAC-2-2-S9, LaCrosse, Wisconsin, USA, 2020, WVA, Molano-Flores, WI-LAC-2-2.

## Literature Cited


Adobe 2019 Adobe Illustrator version 26.5. https://adobe.com/products/illustrator.

Alverson AJ, X Wei, DW Rice, DB Stern, K Barry, JD Palmer 2010 Insights into the evolution of mitochondrial genome size from complete sequences of *Citrullus lanatus* and *Cucurbita pepo* (Cucurbitaceae). Mol Biol Evol 27:1436–1448.

Amos B, C Aurrecoechea, M Barba, A Barreto, EY Basenko, W Bażant, R Belnap, et al 2022 VEuPathDB: the eukaryotic pathogen, vector and host bioinformatics resource center. Nucleic Acids Res 50:D898–D911.

Arthan W, MR McKain, P Traiperm, CAD Welker, JK Teisher, EA Kellogg 2017 Phylogenomics of Andropogoneae (Panicoideae: Poaceae) of mainland Southeast Asia. Syst Bot 42:418–431.

Banerjee AK, W Guo, Y Huang 2019 Genetic and epigenetic regulation of phenotypic variation in invasive plants: linking research trends towards a unified framework. NeoBiota 49:77–103.

Bao W, KK Kojima, O Kohany 2015 Repbase Update, a database of repetitive elements in eukaryotic genomes. Mobile DNA 6:11.

Barrett CF, WJ Baker, JR Comer, JG Conran, SC Lahmeyer, JH Leebens-Mack, J Li, et al 2016 Plastid genomes reveal support for deep phylogenetic relationships and extensive rate variation among palms and other commelinid monocots. New Phytol 209:855–870.

Barrett CF, CD Huebner, ZA Bender, TA Budinsky, CW Corbett, M Latvis, MR McKain, et al 2022 Digitized collections elucidate invasion history and patterns of awn polymorphism in *Microstegium vimineum*. Am J Bot 109:689–705.

Bendich AJ 1993 Reaching for the ring: the study of mitochondrial genome structure. Curr Genet 24:279–290.

Bieker VC, P Battlay, B Petersen, X Sun, J Wilson, JC Brealey, F Bretagnolle, et al 2022 Uncovering the genomic basis of an extraordinary plant invasion. Sci Adv 8:eabo5115.

Camacho C, G Coulouris, V Avagyan, N Ma, J Papadopoulos, K Bealer, TL Madden 2009 BLAST+: architecture and applications. BMC Bioinform 10:421.

Cardi T, P Giegé, S Kahlau, N Scotti 2012 Expression profiling of organellar genes. Pages 323–355 *in* R Bock, V Knoop, eds. Genomics of chloroplasts and mitochondria. Advances in Photosynthesis and Respiration 35. Springer, Dordrecht.

Cavanagh AM, JW Morgan, RC Godfree 2020 Awn morphology influences dispersal, microsite selection and burial of Australian native grass diaspores. Front Ecol Evol 8:581967.

Chen C-H, J-F Veldkamp, C-S Kuoh 2012 Taxonomic revision of *Microstegium* s.str. (Andropogoneae, Poaceae). Blumea 57:160–189.

Chen C-H, JF Veldkamp, C-S Kuoh, C-C Tsai, Y-C Chiang 2009 Segregation of *Leptatherum* from *Microstegium* (Andropogoneae, Poaceae) confirmed by Internal Transcribed Spacer DNA sequences. Blumea 54:175–180.

Clifton SW, P Minx, CM-R Fauron, M Gibson, JO Allen, H Sun, M Thompson, et al 2004 Sequence and comparative analysis of the maize NB mitochondrial genome. Plant Physiol 136:3486–3503.

Crotty SM, BQ Minh, NG Bean, BR Holland, J Tuke, LS Jermiin, AV Haeseler 2020 GHOST: recovering historical signal from heterotachously evolved sequence alignments. Syst Biol 69:249–264.

Daehler CC 1998 The taxonomic distribution of invasive angiosperm plants: ecological insights and comparison to agricultural weeds. Biol Conserv 84:167–180.

Dlugosch KM, FA Cang, BS Barker, K Andonian, SM Swope, LH Rieseberg 2015 Evolution of invasiveness through increased resource use in a vacant niche. Nat Plants 1:15066.

Dlugosch KM, IM Parker 2008 Founding events in species invasions: genetic variation, adaptive evolution, and the role of multiple introductions. Mol Ecol 17:431–449.

Doyle JJ, JL Doyle 1987 A rapid DNA isolation procedure for small quantities of fresh leaf tissue. Phytochem Bull 19:11–15.

Estep MC, MR McKain, D Vela Diaz, J Zhong, JG Hodge, TR Hodkinson, DJ Layton, ST Malcomber, R Pasquet, EA Kellogg 2014 Allopolyploidy, diversification, and the Miocene grassland expansion. Proc Natl Acad Sci USA 111:15149–15154.

Fairbrothers DE, JR Gray 1972 *Microstegium vimineum* (Trin.) *A. Camus* (Gramineae) in the United States. J Torrey Bot Soc 99:97–100.

Fang Y, H Wu, T Zhang, M Yang, Y Yin, L Pan, X Yu, et al 2012 A complete sequence and transcriptomic analyses of date palm (*Phoenix dactylifera L.*) mitochondrial genome. PLoS ONE 7: e37164.

Finch DM, JL Butler, JB Runyon, CJ Fettig, FF Kilkenny, S Jose, SJ Frankel, et al 2021 Effects of climate change on invasive species. Pages 57–83 *in* TM Poland, T Patel-Weynand, DM Finch, CF Miniat, DC Hayes, VM Lopez, eds. Invasive species in forests and rangelands of the United States. Springer, Cham.

Flory SL, F Long, K Clay 2011 Invasive *Microstegium* populations consistently outperform native range populations across diverse environments. Ecology 92:2248–2257.

Frankham R 2005 Resolving the genetic paradox in invasive species. Heredity 94:385–385.

Givnish TJ, M Ames, JR McNeal, MR McKain, PR Steele, CW dePamphilis, SW Graham, et al 2010 Assembling the tree of the Monocotyledons: plastome sequence phylogeny and evolution of Poales. Ann Mo Bot Gard 97:584–616.

Gualberto JM, D Mileshina, C Wallet, AK Niazi, F Weber-Lotfi, A Dietrich 2014 The plant mitochondrial genome: dynamics and maintenance. Biochimie 100:107–120.

Harris RS 2007 Improved pairwise alignment of genomic DNA. PhD diss. Pennsylvania State University, State College.

Hawkins JS, D Ramachandran, A Henderson, J Freeman, M Carlise, A Harris, Z Willison-Headley 2015 Phylogenetic reconstruction using four low-copy nuclear loci strongly supports a polyphyletic origin of the genus *Sorghum*. Ann Bot 116:291–299.

Hoang DT, O Chernomor, A von Haeseler, BQ Minh, LS Vinh 2018 UFBoot2: improving the ultrafast bootstrap approximation. Mol Biol Evol 35:518–522.

Hodgins KA, L Rieseberg, SP Otto 2009 Genetic control of invasive plants species using selfish genetic elements. Evol Appl 2:555–569.

Holec S, H Lange, K Kühn, M Alioua, T Börner, D Gagliardi 2006 Relaxed transcription in *Arabidopsis* mitochondria is counterbalanced by RNA stability control mediated by polyadenylation and polynucleotide phosphorylase. Mol Cell Biol 26:2869–2876.

Hu J, Y Zheng, X Shang 2018 MiteFinderII: a novel tool to identify miniature inverted-repeat transposable elements hidden in eukaryotic genomes. BMC Med Genomics 11:101.

Hudson J, JC Castilla, PR Teske, LB Beheregaray, ID Haigh, CD McQuaid, M Rius 2021 Genomics-informed models reveal extensive stretches of coastline under threat by an ecologically dominant invasive species. Proc Natl Acad Sci USA 118:e2022169118.

Huebner CD 2010*a* Establishment of an invasive grass in closed-canopy deciduous forests across local and regional environmental gradients. Biol Invasions 12:2069–2080.

——— 2010*b* Spread of an invasive grass in closed-canopy deciduous forests across local and regional environmental gradients. Biol Invasions 12:2081–2089.

Huebner CD, CW Corbett, L Ferrari, LE Kosslow, SV Skibicki, CF Barrett 2022 Traits that define invasiveness in *Microstegium vimineum* (Japanese stiltgrass) at local and regional scales. Botany 2022, Anchorage, Alaska.

Hunt M, ND Silva, TD Otto, J Parkhill, JA Keane, SR Harris 2015 Circlator: automated circularization of genome assemblies using long sequencing reads. Genome Biol 16:294.

Jackman SD, L Coombe, RL Warren, H Kirk, E Trinh, T MacLeod, S Pleasance, et al 2020 Complete mitochondrial genome of a gymnosperm, sitka spruce (*Picea sitchensis*), indicates a complex physical structure. Genome Biol Evol 12:1174–1179.

Johnson DJ, SL Flory, A Shelton, C Huebner, K Clay 2015 Interactive effects of a non-native invasive grass *Microstegium vimineum* and herbivore exclusion on experimental tree regeneration under differing forest management. J Appl Ecol 52:210–219.

Kalyaanamoorthy S, BQ Minh, TKF Wong, A von Haeseler, LS Jermiin 2017 ModelFinder: fast model selection for accurate phylogenetic estimates. Nat Methods 14:587–589.

Kassambara A 2020 ggpubr: "ggplot2" based publication ready plots. R package version 0.4.0. https://CRAN.R-project.org/package=ggpubr.

Keller SR, DR Taylor 2010 Genomic admixture increases fitness during a biological invasion. J Evol Biol 23:1720–1731.

Kerns BK, C Tortorelli, MA Day, T Nietupski, AMG Barros, JB Kim, MA Krawchuk 2020 Invasive grasses: a new perfect storm for forested ecosystems? For Ecol Manag 463:117985.

Knoop V, M Unseld, J Marienfeld, P Brandt, S Sünkel, H Ullrich, A Brennicke 1996 Copia-, Gypsy- and LINE-like retrotransposon fragments in the mitochondrial genome of *Arabidopsis thaliana*. Genetics 142:579–585.

Kolbe JJ, RE Glor, L Rodríguez Schettino, AC Lara, A Larson, JB Losos 2004 Genetic variation increases during biological invasion by a Cuban lizard. Nature 431:177–181.

Kolmogorov M, J Yuan, Y Lin, PA Pevzner 2019 Assembly of long, error-prone reads using repeat graphs. Nat Biotechnol 37:540–546.

Koren S, BP Walenz, K Berlin, JR Miller, NH Bergman, AM Phillippy 2017 Canu: scalable and accurate long-read assembly via adaptive *k*-mer weighting and repeat separation. Genome Res 27:722–736.

Kovar L, M Nageswara-Rao, S Ortega-Rodriguez, DV Dugas, S Straub, R Cronn, SR Strickler, et al 2018 PacBio-based mitochondrial genome assembly of *Leucaena trichandra* (Leguminosae) and an intrageneric assessment of mitochondrial RNA editing. Genome Biol Evol 10:2501–2517.

Kurtz S 2001 REPuter: the manifold applications of repeat analysis on a genomic scale. Nucleic Acids Res 29:4633–4642.

Lehwark P, S Greiner 2019 GB2sequin: a file converter preparing custom GenBank files for database submission. Genomics 111:759–761.

Li H, B Handsaker, A Wysoker, T Fennell, J Ruan, N Homer, G Marth, G Abecasis, R Durbin, 1000 Genome Project Data Processing Subgroup 2009 The sequence alignment/map format and SAMtools. Bioinformatics 25:2078–2079.

Lin Y, P Li, Y Zhang, D Akhter, R Pan, Z Fu, M Huang, X Li, Y Feng 2022 Unprecedented organelle genomic variations in morning glories reveal independent evolutionary scenarios of parasitic plants and the diversification of plant mitochondrial complexes. BMC Biol 20:49.

Lloyd Evans D, SV Joshi, J Wang 2019 Whole chloroplast genome and gene locus phylogenies reveal the taxonomic placement and relationship of *Tripidium* (Panicoideae: Andropogoneae) to sugarcane. BMC Evol Biol 19:33.

Ma J, JL Bennetzen 2004 Rapid recent growth and divergence of rice nuclear genomes. Proc Natl Acad Sci USA 101:12404–12410.

Maier RM, P Zeitz, H Kössel, G Bonnard, JM Gualberto, JM Grienenberger 1996 RNA editing in plant mitochondria and chloroplasts. Plant Mol Biol 32:343–65.

Marienfeld J, M Unseld, A Brennicke 1999 The mitochondrial genome of *Arabidopsis* is composed of both native and immigrant information. Trends Plant Sci 4:495–502.

Matheson P, A McGaughran 2022 Genomic data is missing for many highly invasive species, restricting our preparedness for escalating incursion rates. Sci Rep 12:13987.

Minh BQ, HA Schmidt, O Chernomor, D Schrempf, MD Woodhams, A von Haeseler, R Lanfear 2020 IQ-TREE 2: new models and efficient methods for phylogenetic inference in the genomic era. Mol Biol Evol 37:1530–1534.

Mortensen DA, ESJ Rauschert, AN Nord, BP Jones 2009 Forest roads facilitate the spread of invasive plants. Invasive Plant Sci Manag 2:191–199.

Mounger J, ML Ainouche, O Bossdorf, A Cavé-Radet, B Li, M Parepa, A Salmon, J Yang, CL Richards 2021 Epigenetics and the success of invasive plants. Philos Trans R Soc B 376:20200117.

Mower JP, DB Sloan, AJ Alverson 2012 Plant mitochondrial genome diversity: the genomics revolution. Pages 123–144 *in* JF Wendel, J Greilhuber, J Dolezel, IJ Leitch, eds. Plant genome diversity. Vol 1. Plant genomes, their residents, and their evolutionary dynamics. Springer, Vienna.

North HL, A McGaughran, CD Jiggins 2021 Insights into invasive species from whole-genome resequencing. Mol Ecol 30:6289–6308.

Notsu Y, S Masood, T Nishikawa, N Kubo, G Akiduki, M Nakazono, A Hirai, K Kadowaki 2002 The complete sequence of the rice (*Oryza sativa* L.) mitochondrial genome: frequent DNA sequence acquisition and loss during the evolution of flowering plants. Mol Gen Genomics 268:434–445.

Novy A, SL Flory, JM Hartman 2013 Evidence for rapid evolution of phenology in an invasive grass. J Evol Biol 26:443–450.

Ortiz EM 2019 vcf2phylip v2.0: convert a VCF matrix into several matrix formats for phylogenetic analysis. https://doi.org/10.5281/zenodo.2540861.

Palmer JD, LA Herbon 1988 Plant mitochondrial DNA evolves rapidly in structure, but slowly in sequence. J Mol Evol 28:87–97.

Pimentel D, R Zuniga, D Morrison 2005 Update on the environmental and economic costs associated with alien-invasive species in the United States. Ecol Econ 52:273–288.

Poplin R, V Ruano-Rubio, MA DePristo, TJ Fennell, MO Carneiro, GA Van der Auwera, DE Kling, et al 2017 Scaling accurate genetic variant discovery to tens of thousands of samples. bioRxiv 201178.

Ramachandran D, CD Huebner, M Daly, J Haimovitz, T Swale, CF Barrett 2021 Chromosome level genome assembly and annotation of highly invasive Japanese stiltgrass (*Microstegium vimineum*). Genome Biol Evol 13:evab238.

Ranwez V, EJP Douzery, C Cambon, N Chantret, F Delsuc 2018 MACSE v2: toolkit for the alignment of coding sequences accounting for frameshifts and stop codons. Mol Biol Evol 35:2582–2584.

Rauschert ESJ, DA Mortensen, ON Bjørnstad, AN Nord, N Peskin 2010 Slow spread of the aggressive invader, *Microstegium vimineum* (Japanese stiltgrass). Biol Invasions 12:563–579.

Revolinski SR, PJ Maughan, CE Coleman, IC Burke 2023 Preadapted to adapt: underpinnings of adaptive plasticity revealed by the downy brome genome. Comm Biol 6:326.

Rice DW, AJ Alverson, AO Richardson, GJ Young, MV Sanchez-Puerta, J Munzinger, K Barry, et al 2013 Horizontal transfer of entire genomes via mitochondrial fusion in the angiosperm *Amborella*. Science 342:1468–1473.

Rius M, JA Darling 2014 How important is intraspecific genetic admixture to the success of colonising populations? Trends Ecol Evol 29:233–242.

Ruwe H, G Wang, S Gusewski, C Schmitz-Linneweber 2016 Systematic analysis of plant mitochondrial and chloroplast small RNAs suggests organelle-specific mRNA stabilization mechanisms. Nucleic Acids Res 44:7406–7417.

Sakai AK, FW Allendorf, JS Holt, DM Lodge, J Molofsky, KA With, S Baughman, et al 2001 The population biology of invasive species. Ann Rev Ecol Syst 32:305–332.

Sanchez-Puerta MV, LE García, J Wohlfeiler, LF Ceriotti 2017 Unparalleled replacement of native mitochondrial genes by foreign homologs in a holoparasitic plant. New Phytol 214:376–387.

Sedlazeck FJ, P Rescheneder, A von Haeseler 2013 NextGenMap: fast and accurate read mapping in highly polymorphic genomes. Bioinformatics 29:2790–2791.

Simberloff D, J-L Martin, P Genovesi, V Maris, DA Wardle, J Aronson, F Courchamp, et al 2013 Impacts of biological invasions: what's what and the way forward. Trends Ecol Evol 28:58–66.

Sinn BT, CF Barrett 2020 Ancient mitochondrial gene transfer between fungi and the orchids. Mol Biol Evol 37:44–57.

Sinn BT, SJ Simon, MV Santee, SP DiFazio, NM Fama, CF Barrett 2022 ISSRseq: an extensible method for reduced representation sequencing. Methods Ecol Evol 13:668–681.

Sloan DB 2013 One ring to rule them all? genome sequencing provides new insights into the "master circle" model of plant mitochondrial DNA structure. New Phytol 200:978–985.

Sloan DB, Z Wu 2014 History of plastid DNA insertions reveals weak deletion and AT mutation biases in angiosperm mitochondrial genomes. Genome Biol Evol 6:3210–3221.

Smit AFA, R Hubley, P Green 2013 RepeatMasker Open-4.0. http://www.repeatmasker.org.

Soreng RJ, PM Peterson, FO Zuloaga, K Romaschenko, LG Clark, JK Teisher, LJ Gillespie, et al 2022 A worldwide phylogenetic classification of the Poaceae (Gramineae). III. An update. J Syst Evol 60:476–521.

Sutherland BL, CF Barrett, JB Beck, M Latvis, MR McKain, EM Sigel, NJ Kooyers 2021 Botany is the root and the future of invasion biology. Am J Bot 108:549–552.

Turner KG, KL Ostevik, CJ Grassa, LH Rieseberg 2021 Genomic analyses of phenotypic differences between native and invasive populations of diffuse knapweed (*Centaurea diffusa*). Front Ecol Evol 8:577635.

van Boheemen LA, E Lombaert, KA Nurkowski, B Gauffre, LH Rieseberg, KA Hodgins 2017 Multiple introductions, admixture and bridgehead invasion characterize the introduction history of *Ambrosia artemisiifolia* in Europe and Australia. Mol Ecol 26:5421–5434.

Van der Auwera GA, M Carneiro, C Hartl, R Poplin, G del Angel, A Levy-Moonshine, T Jordan, et al 2013 From FastQ data to high-confidence variant calls: the genome analysis toolkit best practices pipeline. Curr Protoc Bioinform 43:11.10.1–11.10.33.

Van der Auwera GA, BD O'Connor 2020 Genomics in the cloud: using Docker, GATK, and WDL in Terra. 1st ed. O'Reilly, Sebastopol, CA.

Verhoeven KJF, M Macel, LM Wolfe, A Biere 2010 Population admixture, biological invasions and the balance between local adaptation and inbreeding depression. Proc R Soc B 278:2–8.

Walker BJ, T Abeel, T Shea, M Priest, A Abouelliel, S Sakthikumar, CA Cuomo, et al 2014 Pilon: an integrated tool for comprehensive microbial variant detection and genome assembly improvement. PLoS ONE 9:e112963.

Watson L, MJ Dallwitz 1992 The grass genera of the world. CAB International, Wallingford, UK.

Weiher E, PA Keddy 1995 The assembly of experimental wetland plant communities. Oikos 73:323–335.

Welker CAD, MR McKain, MC Estep, RS Pasquet, G Chipabika, B Pallangyo, EA Kellogg 2020 Phylogenomics enables biogeographic analysis and a new subtribal classification of Andropogoneae (Poaceae–Panicoideae). J Syst Evol 58:1003–1030.

Wick RR, MB Schultz, J Zobel, KE Holt 2015 Bandage: interactive visualization of *de novo* genome assemblies. Bioinformatics 31:3350–3352.

Wickham H 2016 ggplot2: elegant graphics for data analysis. Springer, New York. https://ggplot2.tidyverse.org.

Wickham H, R François, L Henry, K Müller, D Vaughan 2023 dplyr: a grammar of data manipulation. https://dplyr.tidyverse.org.

Wood DE, J Lu, B Langmead 2019 Improved metagenomic analysis with Kraken 2. Genome Biol 20:257.

Wu Z, JM Cuthbert, DR Taylor, DB Sloan 2015 The massive mitochondrial genome of the angiosperm *Silene noctiflora* is evolving by gain or loss of entire chromosomes. Proc Natl Acad Sci USA 112:10185–10191.

Wu Z, X Liao, X Zhang, LR Tembrock, A Broz 2022 Genomic architectural variation of plant mitochondria: a review of multichromosomal structuring. J Sytematics Evol 60:160–168.

Xiong W, L He, J Lai, HK Dooner, C Du 2014 HelitronScanner uncovers a large overlooked cache of *Helitron* transposons in many plant genomes. Proc Natl Acad Sci USA 111:10263–10268.

Xiong Y, Q Yu, Y Xiong, J Zhao, X Lei, L Liu, W Liu, et al 2022 The complete mitogenome of *Elymus sibiricus* and insights into its evolutionary pattern based on simple repeat sequences of seed plant mitogenomes. Front Plant Sci 12:802321.

Yu X, W Jiang, W Tan, X Zhang, X Tian 2020 Deciphering the organelle genomes and transcriptomes of a common ornamental plant *Ligustrum quihoui* reveals multiple fragments of transposable elements in the mitogenome. Int J Biol Macromol 165:1988–1999.

Zhao N, Y Wang, J Hua 2018 The roles of mitochondrion in intergenomic gene transfer in plants: a source and a pool. Int J Mol Sci 19:547.